On the ocean heat budget and ocean thermal energy conversion

Mohammed Faizal, M. Rafiuddin Ahmed

Division of Mechanical Engineering, the University of the South Pacific, Laucala Campus, Suva, Fiji Islands

SUMMARY

Ocean water covers a vast portion of the earth's surface and is also the world's largest solar energy collector. It plays an important role in maintaining the global energy balance as well as in preventing the earth's surface from continually heating up due to solar radiation. The ocean also plays an important role in driving the atmospheric processes. The heat exchange processes across the ocean surface are represented in an ocean thermal energy budget, which is important because the ocean stores and releases thermal energy. The solar energy absorbed by the ocean heats up the surface water, despite the loss of heat energy from the surface due to back-radiation, evaporation, conduction and convection, and the seasonal change in the surface water temperature is less in the tropics. The cold water from the higher latitudes is carried by ocean currents along the ocean bottom from the poles towards the equator, displacing the lower density water above and creating a thermal structure with a large reservoir of warm water at the ocean surface and a large reservoir of cold water at the bottom, with a temperature difference of 22ºC to 25ºC between them. The available thermal energy, which is the almost constant temperature water at the beginning and end of the thermocline, in some areas of the oceans, is suitable to drive ocean thermal energy conversion (OTEC) plants. These plants are basically heat engines that use the temperature difference between the surface and deep ocean water to drive turbines to generate electricity. A detailed heat energy budget of the ocean is presented in the paper taking into consideration all the major heat inputs and outputs. The basic OTEC systems are also presented and analyzed in this paper.

KEY WORDS: Ocean heat budget; Thermocline; Ocean thermal energy conversion (OTEC)

1. INTRODUCTION

The Earth's surface is approximately covered by seventy percent of water. Ocean water makes up 97.4% of the total water available [**1**]. The global-ocean can be classified as a continuous body of water that separates into several major oceans and seas [**2**]. The major ocean divisions, according to their size, are the Pacific Ocean, Atlantic Ocean, Indian Ocean, Southern Ocean, and the Arctic Ocean [**2,3**]. The average temperatures of the ocean waters hardly exceed 30ºC or reduce below -2ºC [**4**]. It is the water in the oceans that prevents wide variations of temperature on the Earth's surface globally [5]. Moreover, the Earth is the only planet in the solar system with oceans [**6**]. The processes that control the atmosphere are closely related to the ocean processes. Changes in weather and climate are a result of the interaction between the Sun, the atmosphere, and the water on the Earth's surface [**7**].

Water has the highest heat capacity when compared to any other fluid. The amount of heat energy required to raise the temperature of a given mass of water by 1ºC is more than that of other fluids [**8**]. Moreover, the ocean has the largest heat capacity compared to any single component of the climate system [**9**]. This property of water allows a lot of solar energy to be stored in the oceans, thus preventing the Earth's surface from heating up [**5**]. The major source of thermal energy entering the ocean is from the Sun. The ocean plays an important role in maintaining the global energy balance of the Earth's atmosphere. The ocean stores thermal energy to a much greater extent than land because of its high heat capacity [**10**]. The ocean can absorb heat in one region and restore it in a different place, even after decades or centuries [**11**]. The amount of thermal energy entering the ocean must be equal to the thermal energy leaving or the average temperature of the ocean will change [**12**]. Significant heat exchange processes across the ocean surface are represented in an ocean energy budget [**13**]. The ocean energy budget is important because the ocean stores and releases much more heat than the land over different seasons [**14**], thus preventing the Earth from heating up.

The thermal energy in the oceans is distributed around the globe by moving ocean currents [**15**]. The waters of the ocean are continuously moving. Whereas winds are described in terms of where they are blowing *from*, ocean currents are described in terms of where they are blowing *towards* [**11**]. The circulation of waters in the oceans helps to distribute the thermal energy in the lower latitudes to certain areas in higher latitudes, thus modifying climate conditions [**16**]. The equatorial regions, or the lower latitudes, receive much more heat from the Sun than the polar regions because of the different angles at which the sunlight strikes the Earth [**5**]. The major factors that drive the ocean currents are solar energy and the Earth's rotation [**17**]. Atmospheric winds derive energy from the Sun and this energy is transferred to the upper layers of the ocean by tangential stress on the ocean surface, thus setting the surface water in motion in the direction of the wind. The rotation of the Earth alters the direction of the ocean currents driven by atmospheric winds [**17**]. Solar energy that is directly absorbed by the ocean varies from region to region due to unequal heating of the Earth's surface [**4**]. This leads to variations in density by affecting the temperature and salinity through heating, evaporation, and precipitation. The density differences between bodies of water in different regions (mainly at the equator and the poles) give rise to a density driven circulation of deep water currents known as the thermohaline circulation [**17**]. Different flow profiles and reference temperatures affect the possible values of heat transfer by ocean currents [**18**]. Ocean circulation is not driven by thermal energy due to temperature differences in different locations [19]. However, thermal circulation is created in oceans by differential heating through the surface causing density differences which are then acted upon by gravitational forces [**20**].

The temperature of the ocean waters generally decreases with increasing depth, except for polar regions [**8,21**]. The surface layer of the oceans is usually referred to as the *mixed layer*, because the near-surface waters are well mixed by winds and waves and a nearly isothermal condition is maintained [**4,22**]. Below the mixed layer is a region of rapidly changing temperature known as the *thermocline*. It is this region that separates the upper mixed layer of the ocean with deep ocean water [**23**]. Its characteristics vary with season, latitudes, environmental conditions and ocean currents. The thermocline is the deepest in

the tropics and shallower in the polar regions [**24**]. Below the thermocline, is a region of deep cold ocean water where the temperature reaches an almost isothermal condition [**25**]. The deep cold ocean water is transferred from the polar latitudes [**17,22**]. The surface water thus acts as a large reservoir of warm water and the deep water (approximately at 1000 m) acts as a large reservoir of cold water in the tropical oceans throughout the year [**22**]. This uniform temperature difference can be used to operate Ocean Thermal Energy Conversion (OTEC) plants [**26**]. This is one of the many renewable energy technologies available. Possible solutions to problems associated with high CO_2 emissions are energy conservation through improved, energy efficient products and increased use of renewable energy sources and technologies [**27**].

Ocean thermal energy conversion (OTEC) is a technique that utilizes the temperature difference between warm surface water and deep cold water of the ocean to operate a low pressure turbine [**22,28**]. An OTEC power plant acts as a heat engine that extracts energy as heat from the warm surface water, converts part of that energy to generate electricity and rejects the remaining energy as heat to the cold deep sea water in a cyclic process [**22,27**]. It is a thermodynamic phenomenon and is in the category of green engineering related to energy. In thermodynamics, the concept of green can be associated with an energy source, an energy transfer, and energy conversion process. An energy source that can be use to do work with minimal adverse impact on the environment and the future supplies can be viewed as green. With this definition, clean, renewable and sustainable energy like ocean thermal energy is green energy, but fossil fuels are not [**29**]. OTEC plants can be integrated with a desalination plant, commonly known as the hybrid cycle, to produce fresh water [**30,31**]. An OTEC plant is more suitable for low latitudes (tropical oceans) because the water temperature remains almost uniform throughout the year with few variations due to seasonal effects [**28**]. About 63% of the surface of the tropics between latitudes 30ºN and 30ºS is occupied by ocean water [**32**]. Solar energy that is absorbed by the tropical oceans maintains a relatively stable surface temperature of 26-28ºC to a depth of approximately 100 m. As the depth increases, the temperature drops, and at depths close to 1000 m, the temperature is as low as 4ºC. Below this depth, the temperature drops only a few degrees.

Pacific Island countries have a lot of potential for implementation of OTEC technologies because of the high ocean temperature gradient. Apart from generating electricity and producing fresh water, OTEC plants can be utilized for other benefits such as production of fuels such as hydrogen, ammonia, methanol, providing air-conditioning for buildings, on-shore and near-shore mariculture, and extraction of minerals [**33-35**].

2. THE OCEAN ENERGY BUDGET

The ocean energy budget is an expression of the first law of thermodynamics for an incompressible fluid, where the rate of change of the internal energy of the system is equal to the net heat flux through the boundaries of the system. The internal energy is represented by the temperature structure of the ocean [**36**]. The ocean heat budget consists of thermal energy gains and losses [**37**]. The total thermal energy entering the ocean must equal the total thermal energy lost or the average ocean temperature will change over a certain period which will lead to significant warming or cooling trends [**38**]. Apart from solar energy, the other forms of thermal energy available to the ocean are from conduction through the ocean bottom from the Earth's interior, heating and cooling from chemical and biological processes, heat generated from friction developed due to moving ocean currents, and heat gain from decay of radioactive matter in the ocean [**37**]. But these processes are mostly neglected in the ocean heat budget because of their small magnitude compared to solar energy input [**36**]. It can be assumed that all the heat exchange processes occur at the surface of the ocean [**11,39**], where the ocean is the thermodynamic system and the surface is the boundary between the ocean and the atmosphere.

As solar energy enters the atmosphere, some energy is scattered, some is absorbed or reflected by clouds, and some is reflected or absorbed by the ocean, land, and ice on the Earth's surface [**8**]. Variations in cloud cover over different regions causes the largest variation in the amount of solar energy reaching the Earth's surface [**8, 40**]. Heat is exchanged across the ocean *surface* by four significant processes [**12,14**]:

i) short wave radiation from the Sun; ii) heat loss due to long-wave back radiation; iii) latent heat loss as the water at the surface is evaporated; iv) sensible heat transfer due to conduction or heat exchange between ocean and atmosphere as a result of temperature difference between the sea surface and the atmosphere

Apart from the energy interactions at the ocean surface, thermal energy is also distributed *within* the ocean by currents and mixing. Ocean currents transport thermal energy from low to high latitudes by advection. The loss of thermal energy from low latitude regions to high latitude regions ensures that the low latitude regions do not continually heat up and the high latitude regions do not continually cool down [**41**]. Thermal energy lost by the tropical regions to cooler regions also drives the atmospheric circulation [**42**].

The principal forms of heat transfer in a given area of the ocean are represented in Figure 1.The rate of heat gain or lost, $\dot{Q}_T$, by a given vertical column of ocean water with a unit horizontal cross sectional area [**43**] can be expressed as the difference between the total heat coming from the Sun and the total thermal energy loss from the given area. The rate of heat absorbed by the ocean from incoming solar radiation is $\dot{Q}_s$, the rate of heat loss by back radiation is $\dot{Q}_b$, sensible heat loss by convection and conduction is $\dot{Q}_h$, rate of heat loss (latent heat) by evaporation from the ocean surface is $\dot{Q}_e$, and $\dot{Q}_v$ is the thermal energy transported by ocean currents moving out of the given area [**4,36,39**]. The heat and thermal energy interactions mentioned in the present paper are all the rates of such interactions.

The generally accepted formal sign convention for heat interaction is that heat transfer *to* a system is positive and heat transfer *from* a system is negative [**44**]. The heat transfer terms in Figure 1 can be represented by an equation according to the conservation of energy principle [**4, 36, 43**]:

$$\dot{Q}_T = \dot{Q}_s - \dot{Q}_b - \dot{Q}_h - \dot{Q}_e - \dot{Q}_v \tag{1}$$

The $\dot{Q}_h$, $\dot{Q}_b$, and $\dot{Q}_v$ terms in equation 1 could be either positive or negative depending on whether thermal energy is gained or lost by the given area [**39,40**]. The term in equation 1 that transfers thermal energy from one region of the ocean to another is $\dot{Q}_v$, stating the effects of ocean currents [**40**]. However, for the ocean as a whole, $\dot{Q}_v$ is taken as zero because it only accounts for the redistribution of thermal energy *within* the ocean [**4,40**]. There is a net gain of thermal energy throughout the year in the lower latitudes (positive $\dot{Q}_T$), but a net gain in summer (positive $\dot{Q}_T$) and a net loss (negative $\dot{Q}_T$) in winter in the higher latitudes [**43,45**].

The rate of heat gain (or loss) by a given area of the ocean is normally averaged over an year. Therefore, the amount of heat *available* for heating a given area of the ocean over any period, *t*, (taking $\dot{Q}_v$ = 0) is [**12**]:

$$\int_0^t \dot{Q}_T .dt = \int_0^t \left(\dot{Q}_s - \dot{Q}_b - \dot{Q}_h - \dot{Q}_e\right)dt \qquad (2)$$

The distribution of the heat in the surface layer can also be calculated [**12, 46**]. A heat budget can also be applied to the surface layer (or mixed layer) of the oceans [**47,48**].

2.1.Rate of heat added by short-wave solar radiation ($\dot{Q}_S$)

The solar radiation that reaches the ocean surface is in the form of direct solar radiation and indirect diffused sky radiation [**49**]. The sky radiation results from scattering due to the presence of molecules in the Earth's atmosphere [**50**] which causes the solar energy to reach the Earth's surface as diffused sunlight. The incoming radiation is termed as short wave because about 99% of the solar radiation [**39**] is in the visible and near-visible parts of the electromagnetic spectrum with wavelengths of approximately 0.4 to 4 μm [**51**]. The incoming radiation is affected by the altitude of the Sun, cloud cover, latitude, time of the day, the season, and by the geographical location [**52**].Solar radiation intensity is

greatest at the equator, moderate at middle latitudes, and lowest at the higher latitudes (poles) [**45**]. As shown in Figure 2, different regions on the Earth's surface that are equal in size receive different levels of solar radiation. The solar radiation intensity is largest between 23.5 ºN and 23.5 ºS because the sunlight strikes at a right angle between these latitudes, shown in Figure 2a [**53**]. Higher latitudes receive less solar energy compared to the equator because of the decreasing angle at which the sunlight strikes the Earth's surface [**5**]. Also, the sunlight has to travel a larger distance through the atmosphere at higher latitudes (Figure 2d), thus the atmosphere absorbs most of the solar radiation intensity before it reaches the Earth [**53**].

At any given time, the Earth receives solar energy equal to the solar constant minus the amount of shortwave radiation reflected back into space, times the cross-sectional area of the Earth that is perpendicular to the beam of parallel solar radiation [**54**]. Solar constant can be defined as the rate at which the Earth receives radiant energy from the Sun on an area perpendicular to the Sun's rays, measured at a point beyond the Earth's atmosphere when the Earth is at its mean distance from the Sun [**55**]. The solar constant is approximately equal to 1.94 calories per minute per square centimeter of area perpendicular to the Sun's rays [**55**].

Figure 3 shows a division of 100 units of short-wave radiation from the Sun entering the atmosphere and how it gets absorbed and scattered in various ways, representing a long-term world-area average. Of the total incoming radiation units, about 29 parts are lost to space by scattering from the atmosphere and the clouds. About 19 parts are absorbed in the atmosphere and the clouds, and about 4 parts are reflected to space from the sea surface. The remaining units enter the ocean, from which a small part is scattered upwards, and the remainder represents the $\dot{Q}_S$ term of the heat budget (equation 1) [**56**].

After scattering in the water, a small part of the solar radiation radiates back in the form of diffused underlight. The greatest part is absorbed by the water [**49**]. Of the total 48 parts absorbed by the ocean, about 29 parts reach the ocean as direct solar radiation, whereas 19 parts from indirect scattered radiation from the atmosphere [**56**].

The absorbed energy heats up the surface water of the oceans and the surface layer undergoes a temperature cycle similar to the atmosphere. The seasonal temperature change is generally smaller in the tropics than in higher latitudes (disregarding upwelling, seasonal current shifts, coastal effects, and advection) [**8**]. The incoming solar radiation is absorbed gradually as it goes below the ocean surface [**57**]. The rate at which $\dot{Q}_S$ enters the surface of the ocean and is available to raise the water temperature depends on the Sun's elevation, amount of sunlight reflected, and the amount that gets transmitted into the water [**56**].

The intensity of incoming solar radiation on the ocean surface can be measured from ships or coastal stations. A pyranometer or a solarimeter is a sensor that is used to measure the incoming solar radiation [**58,59**]. Also, estimates can be made from tables giving radiation from a cloudless sky, as a function of the latitudes and the time of the year, with correction factors for cloud covers [**43**]. A simple approximation to calculate short-wave radiation penetrating the sea after taking into account the atmospheric factors and back radiation from the ocean surface is presented in [**56,60**]. The short-wave radiation input averaged over 24 hours in the absence of clouds and allowing for atmospheric loss is given as [**56**]:

$$\dot{Q}_{so} = 0.4 A_n t_d \tag{3}$$

where A_n is the noon altitude of the Sun in degrees, t_d is the length of the day in hours from sunrise to sunset. To calculate the back radiation from the ocean surface, the cloud cover, C (measured in Oktas), is taken into account. The sky conditions are estimated by how many eighths (or tenths) of the sky are covered by clouds, C = 0 meaning completely clear and C = 8 meaning completely overcast [**61**]. The term $\dot{Q}_S$ is actually the difference between the rate at which solar radiation is received at the ocean surface and the reflected radiation from the ocean surface [**39**]. The amount of short-wave radiation received by the surface of the ocean after cloud obstructions, $\dot{Q}_S'$, is approximated as [**56,60**]:

$$\dot{Q}_S' = \dot{Q}_{so}\left(1 - 0.0012C^3\right) \tag{4}$$

The amount of short-wave radiation reflected from the ocean surface, $\dot{Q}_r$, is approximated as:

$$\dot{Q}_r = 0.15\dot{Q}_S' - (0.01\dot{Q}_s')^2 \tag{5}$$

Finally, $\dot{Q}_s$, which is the difference between $\dot{Q}_S'$ and $\dot{Q}_r$, is approximated as:

$$\dot{Q}_S = \dot{Q}_S' - \dot{Q}_r \tag{6}$$

These equations are approximations. To get comparable results, recorded tabulated values over a long period should be used.

2.2. Rate of heat loss due to long-wave back radiation ($\dot{Q}_b$)

The reflection of the incoming radiation at the ocean surface depends on the altitude of the Sun and the state of the ocean surface described by the ocean waves [**49**]. Figure 4 shows the reflection of solar radiation from the ocean surface at different altitudes for smooth and actual ocean surfaces. At Sun altitudes of over 40º, less than 5% of the solar radiation is reflected back from the surface, thus, showing that there is almost complete solar radiation absorption at the ocean surface in those regions. The reflection of solar radiation at the ocean surface increases with decreasing altitudes of the Sun, thus, explaining the cold regions towards the poles [**49**]. The percentage of the energy reflected is called the albedo, and the albedo is higher over lighter areas such as snow and lower over darker areas such as the oceans [**62**].

All bodies with a temperature above absolute zero radiate heat. The amount is proportional to the fourth power of the absolute temperature, *T*, given by Stefan-Boltzmann law. The ocean surface radiates heat as a black body having the same

temperature of the surface water, which is approximately 290 K [**14**]. Much of the back radiation from the ocean surface is affected by the presence of clouds and water vapor in the atmosphere, which absorbs and re-radiates the heat back to the ocean surface [**14**]. The effective back radiation from the ocean surface, $\dot{Q}_b$, therefore, is the difference between the outward radiation from the ocean surface and the downward radiation (re-radiation) from the atmosphere [**39**]. The back radiation from the ocean surface is termed as long-wave radiation because the electromagnetic wavelength has a value of 10μ, which falls in the long-wave heat radiation range (3 to 80 μm) [**49, 56**]. The $\dot{Q}_b$ term depends on the ocean surface temperature, humidity of the atmosphere, and the cloud cover [**43**]. In the presence of clouds, $\dot{Q}_b$ is reduced because the downward radiation from the atmosphere is increased.

The long-wave back radiation from the ocean surface, $\dot{Q}_b$, can be measured using a radiometer, which is a device that measures the radiant flux of electromagnetic radiation [**63**]. Also, estimates can be made from formulas by taking into account the sea surface temperature, humidity of atmosphere, and the cloud cover [**43**]. The Stefan-Boltzmann law in its original form cannot be applied to calculate the theoretical back radiation from the ocean surface. If used in its original form, it would appear that the ocean surface loses more energy than it receives [**12**]. The factors that affect back radiation such as clouds and water vapor in the atmosphere have to be taken into account [**8**]. Equation 7 is an empirical formula that calculates the effective back radiation in cal. per cm^2.per minute [**49**]:

$$\dot{Q}_b = \sigma T^4 \left[1 - \left(0.210 + 0.174 \times 10^{-0.055 e_o} \right) (1 - 0.765C) \right] \tag{7}$$

where σ is the Stefan-Boltzmann constant, T is the absolute temperature (which can be equal to the water temperature), e_o is the water vapor pressure over the ocean surface in millibars, and C is the mean cloudiness in tenths of sky coverage. A similar approximation is provided in ref. [**39**].

An evaluation of the incoming solar radiation, $\dot{Q}_s$, and back radiation, $\dot{Q}_b$, at the ocean surface shows that there is more solar energy coming from the Sun at all latitudes on an annual average when compared to back radiation [**49**]. This radiation balance is much more over the ocean surface compared to land [**12**].

2.3. Rate of heat loss by evaporation ($\dot{Q}_e$)

Evaporation is the largest contributing factor to the overall thermal energy losses from the ocean surface [**8**]. On a yearly average, about 120 cm of water is evaporated from the ocean surface [**56**]. When evaporation occurs, there is an increase in salinity at the ocean surface, and precipitation, conversely, decreases salinity. This affects the density of the surface water [**64**], which can be accounted for in an ocean salinity budget. The rate of heat loss by the ocean surface from evaporation is gained by the atmosphere in the form of latent heat. This heat is released from the atmosphere by the condensation of water vapor [**65**]. Ninety percent of the radiative heating of the global ocean is balanced by evaporation from the ocean surface [**66**].

The ocean surface is usually a degree or two warmer than the air directly above it [**12**]. Evaporation takes place when the air close to the ocean surface becomes unsaturated with water vapor. The air becomes unsaturated with water vapor by the heating from the ocean surface (ocean surface is warmer than the air directly above it) [**49**]. The higher the temperature of this air, the more water vapor it can absorb [**67**]. As long as the sea temperature is more than about 0.3 K greater than the air temperature, there will be heat lost from the ocean to the atmosphere due to evaporation [**56**]. The heat transfer from the ocean surface to the lowest atmospheric layers that are very close to the ocean surface causes the air to become unstable and to be convected upwards [**68**]. The cooler drier air replaces the upward moving warmer air, and becomes saturated with water vapor as evaporation continues at the ocean surface. These small convection processes remove the air saturated with water vapor and allow it to be replaced with unsaturated air which accepts more moisture through evaporation [**12**]. Condensation occurs when the air at a certain temperature blows over water that is cooler. When thermal energy is lost from the

air close to the ocean surface, the air becomes stable and less turbulent. Therefore, the thermal energy gained by the ocean from condensation is very small compared to the loss of latent heat by evaporation [**49**]. The wind speed over the ocean surface also enhances evaporation because it gives rise to turbulent transfer processes. The winds generate waves on the surface of the ocean and turbulence in the air close to the ocean surface [**69**]. Strong winds lead to breaking waves from which spray is formed, thus enhancing evaporation [**70,71**]. Waves break when the wave height exceeds the wavelength by a ratio of 1:7 [**53**].

The rate of evaporation from the ocean surface varies at different latitudes and seasons [**72**]. As shown in Figure 5, the atmosphere at higher latitudes is less capable of absorbing water vapor because of the low air temperatures close to the ocean surface, thus, the evaporation is less compared to lower latitudes. At the equator (0º), the air is already saturated with water vapor, therefore, evaporation is smaller in comparison to 20º [**49**]. Also, the wind velocities are small close to the equator due to the Cariolis force being zero [**73**].

The rate of latent heat loss by evaporation from the sea surface is estimated based on the vapor pressure at the ocean surface, the actual vapor pressure in the air at a height of 10 m above ocean surface, and the wind speed at 10 m height [**12,49**] . The rate of latent heat loss from the ocean surface, $\dot{Q}_e$, due to evaporation is given as [**56**]:

$$\dot{Q}_e = F_e . L_t \tag{8}$$

where F_e is the rate of evaporation of water in kg/s per square meter of sea surface, and L_t is the latent heat of evaporation in kilojoules for a given mass. The value of L_t for pure water depends on the water temperature, and is given as [**56**]:

$$L_t = (2494 - 2.2T) \tag{9}$$

The rate of evaporation of water, F_e, is approximated by taking into account the eddy diffusivity of water vapor, A_e, which depends on the turbulence character of water, and the gradient of water vapor concentration in the air above the ocean surface, de/dz [**56**].

$$F_e = -A_e . \frac{\mathrm{d}e}{\mathrm{d}z} \tag{10}$$

An empirical formula is mostly used to estimate the rate of evaporation from the ocean surface. Taking into account the wind speed and substituting equations 9 and 10 into equation 8, the empirical formula obtained is [**56**]:

$$\dot{Q}_e = 1.4(e_s - e_a).W.(2494 - 2.2T_s).10^{-3} \tag{11}$$

where e_s is the saturated water vapor pressure at the surface, e_a is the actual vapor pressure at a height of 10 m above the surface (both in kPa), and W is the wind speed in m/s at a height of 10 m above the sea level. A similar empirical estimation is provided by Jacob in ref. [**12**].

2.4. Rate of sensible heat loss ($\dot{Q}_h$)

The rate of heat loss by conduction and convection from the ocean surface depends on the temperature gradient between the ocean surface and the air. On the average, the surface temperature of the ocean is higher than the lowest atmospheric layers [**12**]. Convection occurs due to the air close to the ocean surface being heated. The lowest part of the atmosphere close to the ocean surface gets heated and becomes unstable. A vertical convection occurs in the atmosphere, and air masses heated by the ocean surface get replaced by cooler air masses from the upper atmosphere. The air at the ocean surface expands and rises in the atmosphere, thus carrying heat away from the surface [**12,49**].

The surface heat fluxes of the ocean-atmosphere coupling have regional and seasonal variations [**74**]. The heat transfer from the water to the air is more significant than the

reverse because at equal temperatures, the heat capacity of water is much higher [**8**]. The conduction terms of the ocean heat budget are calculated from equations which involve the difference between the ocean surface temperatures, T_s, and the air temperature, T_a, at a standard height above the ocean surface, and the wind speed W [**43**]. The rate of heat loss is, however, not controlled by molecular forces [**12**]. The heat transfer increases with increasing wind speed, where as a high speed increases turbulence across the ocean-atmosphere interface [**68**]. Heat transfer by conduction is proportional to the vertical temperature gradient in the lowest atmospheric layer, dt/dz, the eddy conductivity, A_h, and the specific heat of air at constant pressure, C_p. [**49,56**]:

$$\dot{Q}_h = -C_P.A_h \,\mathrm{dt/dz} \tag{12}$$

Wyrtki, in ref. [**56**], simplified this equation to calculate the heat budget for the Pacific Ocean, given as:

$$\dot{Q}_h = -1.88.W.(T_s - T_a) \tag{13}$$

The rate of sensible heat loss or conduction, $\dot{Q}_h$, and the latent heat loss by evaporation, $\dot{Q}_e$, varies together over the ocean surface due to climatic variations. It can therefore be said that the ratio, $\frac{\dot{Q}_h}{\dot{Q}_e}$, known as the *Bowens ratio, B*, remains almost constant [**40**]. Considering equation 1, and taking $\dot{Q}_V$ and $\dot{Q}_T$ to be zero, (no advection and steady state), and substituting *B*:

$$\dot{Q}_e = \left(\frac{\dot{Q}_s - \dot{Q}_b}{B+1} \right) \tag{14}$$

The Bowen's ratio is also calculated by using the temperatures and the vapor pressures, and by assuming that A_e and A_h are numerically similar [**12,54**]:

$$B = 0.062 \left(\frac{T_s - T_a}{e_s - e_a} \right) \tag{15}$$

The Bowen's ratio increases with latitude for both land and oceans [64]. The average value of B at the equator is 0.1 [**40**]. Figure 6 shows the $\dot{Q}_h$ and $\dot{Q}_e$ terms at different latitudes.

2.5. Thermal energy transport by ocean currents ($\dot{Q}_V$)

In lower latitudes, there is a radiation surplus of the Earth-atmosphere system which decreases with increasing latitude [**45**], as shown in Figure 7. The surplus thermal energy at the lower latitudes is transported to higher latitudes by ocean currents, maintaining an even temperature distribution [**62,75**]. The temperature of a given location in the atmosphere or in the ocean, averaged over several years is nearly constant. Long term climatic changes are negligible compared to daily and seasonal changes. Advection plays a major role in the overall heat energy balance of the ocean. Changes in the oceanic circulation will affect the overall ocean-atmosphere heat energy balance by affecting weather patterns, since ocean currents are also driven by atmospheric winds [**12**].

The amount of radiation received at different latitudes is different because of different angles at which sunlight strikes the Earth, discussed in section 2.1. The $\dot{Q}_V$ term in the heat budget (equation 1), or advection ensures that the low latitudes do not continually heat up and the high latitudes do not continually cool down [**40**]. Because of its higher density and minimal mixing with the warmer water of the surface, the cold water from the higher latitudes is carried by ocean currents along the ocean bottom from the poles towards the equator, displacing the lower density water above. These two physical processes create a thermal structure with a large reservoir of warm water at the ocean surface and a large reservoir of cold water at the bottom, with a temperature difference between them of 22ºC to 25ºC [**22**]. The thermal structure of the oceans is discussed in section 3.1. For the ocean as a whole, $\dot{Q}_V$ is taken as zero because it takes into account the redistribution of thermal energy *within* the ocean [**4,40,49**]. Ocean circulation accounts for 40% of the latitudinal heat transfer from the equator to the poles, whereas the remaining 60% heat transfer occurs through the atmosphere [**76**].

Accurate measurements and prediction of the amount of thermal energy in the oceans remains a difficult task. Zhang et al. [**77**] studied 1 - 2 decades of radiative flux data sets, ocean surface turbulence flux data sets, and ocean thermal energy data sets and found that even though there are some imbalances, the data sets show excellent quantitative agreement. Studies done by Josey et al. [**38**] show that there are some imbalances of the overall energy budget, but they attribute this to possible errors in flux equations. Together with an oceanic thermal energy balance, there is a salt and water balance. The amount of water that is evaporated from the ocean surface is replaced by water from rainfall and river runoff [**78**]. A conservation of volume analysis based on evaporation and precipitation is shown in ref. [**56**]. Salt is left behind when ocean water evaporates. Coastal regions have lower salinities because of water coming from rivers [**4**]. The average salinity of the oceans remains almost constant [**54**], and it would be hundreds of years before an increase in the salinity is detected if all the salts are brought into the oceans from rivers [**12,56**].

The rate of heat addition to the ocean by short-wave radiation is highest in the equatorial regions and varies with different latitudes and seasons. The rate of heat loss by back radiation from the ocean surface increases with decreasing altitudes of the Sun. The rate of latent heat loss by evaporation from the ocean surface is the largest contributing factor to the overall heat losses from the ocean and is higher close to the equator and decreases with increasing latitudes. The rate of heat loss by convection and conduction varies with seasons and latitudes, and depends on the temperature difference between the ocean surface and the air close to the surface. Ocean currents transfer thermal energy from the lower latitudes to cooler regions in the higher latitudes, ensuring that the lower latitudes do not continually heat up or the higher latitudes do not continually cool down. The ocean heat budget quantifies the amount of thermal energy gained and lost by the ocean, and this can be used to determine the overall temperature change of the system over a certain period of time. The transport of cold water from the higher latitudes towards the equator along the ocean bottom results in the displacement of the lower density water above and creates a thermal structure with a large reservoir of warm water at the ocean surface and a large reservoir of cold water at the bottom, with a temperature difference

between them of 22ºC to 25ºC. This temperature difference can be used to drive an ocean thermal energy system.

3. OCEAN THERMAL ENERGY CONVERSION (OTEC)

An ocean thermal energy conversion (OTEC) plant is basically a heat engine that utilizes the temperature difference between the warm surface water and deep cold sea water to produce electricity [**28**]. From the view of a thermodynamicist, any temperature difference can be used to generate power [**22**].

The technology for OTEC was first proposed by Jacques d'Arsonval, in the year 1881 in France [**79,80**]. He proposed a closed cycle OTEC design that used ammonia as the working fluid [**81**]. However, it was his student, George Claude who built the first OTEC plant in Cuba in 1930 [**82**]. A low pressure turbine was used to generate 22 kW of electricity for a short while before the system got damaged [**83**]. Ocean thermal energy is a potential source of renewable energy and with proper designing, it could provide a source of clean renewable energy with constant power output with many other benefits such as pure drinking water, which can benefit many small island countries and developing countries [**84**]. An OTEC system in its simplest form contains three basic constituents: an energy supply source, a power generation system, and a possible desalination system [**85**].

Ocean thermal energy conversion power systems are basically divided into three categories: open cycle, closed cycle, and hybrid cycle. An open cycle OTEC system utilizes the warm surface water as the working fluid. The surface water is pumped into a chamber where a vacuum pump reduces the pressure to allow the water to boil at low temperature to produce steam. The steam drives a turbine coupled to a generator and then is condensed (using deep cold seawater pumped to the surface) to produce desalinated water [**22, 86**]. A closed cycle OTEC system incorporates a working fluid, such as Ammonia or Ammonia/Water mixture, operating between two heat exchangers in a closed cycle. A closed cycle utilizes the warm surface water to vaporize the working fluid

in a heat exchanger (evaporator). The vaporized fluid drives a turbine coupled to a generator. The vapor is then condensed in a heat exchanger (condenser) using cold deep seawater pumped to the surface. The condensed working fluid is pumped back to the evaporator where vapor is generated and the cycle is repeated. The thermodynamic principles of the open cycle and the closed cycle are similar [**22,87**]. The cycles are basic Rankine cycles that operate between a heat source and sink to generate electricity [**88,89**] with efficiencies close to 3% [**88**]. To increase the thermal efficiency of the OTEC system, other kinds of energies such as solar energy, geothermal energy, industrial waste energy, and solar ponds can be introduced to increase the temperature difference [**90-92**]. Preheating of the feed water is also done in commercial plants operating on Rankine cycles, such as fuel-fired plants, to improve the efficiency [**93**]. Major differences between the open and closed cycle systems are the sizes of ducts and turbines, and the surface area required by heat exchangers for effective heat transfer [**22**]. For a given OTEC system with a certain power output, a closed cycle system with ammonia as the working fluid requires a much smaller duct and turbine diameter compared to an open cycle system which has water as the working fluid [**94**]. The difference is attributed to the pressure difference across the turbine and the specific volume of the working fluids. The heat exchangers for closed cycle systems require large surface areas to have effective heat transfer [**22**].

The hybrid system integrates the power cycle with desalination to produce electricity and desalinated water. Nearly 2.28 million liters of desalinated water can be obtained everyday for every MW of power generated by a hybrid OTEC system [**95**]. Electricity is generated in the closed cycle system circulating a working fluid and the warm and cold seawater discharges are passed through the vacuum chamber and condenser to produce fresh water [**22**]. The power that the pumps need to do work is supplied from the gross power output of the OTEC power generating system. The hybrid cycle eliminates the use of a large low-pressure turbine as is required by an open cycle. The vacuum chamber is also reduced in size [**22**]. The working fluids for either closed or hybrid cycles should be such that the system is able to operate between the low temperatures and still give optimum efficiency. Mostly Freon and ammonia are used, whereas ammonia and water

mixture are also accepted for use [**96**]. The use of mixtures instead of one component fluid improves the thermodynamic performance of power cycles [**97**]. Studies done by Kim et al. [**98**] suggest that working fluids can be selected based on the specific environment and working conditions without affecting the efficiency much.

An energy harnessing scenario involves three steps: i) determining the activities in the target society that requires energy, ii) determining the available energy resources, and iii) matching the demand and the supply [**99**]. Moreover, even though the thermal resource is available to many countries, there are many factors that must be taken into account before a particular country or location is selected for an OTEC plant installation. Some of them are: distance of the thermal resource from land; depth of the ocean bed; depth of the resource; size of the thermal resource within the exclusive economic zone (EEZ); replenishment capability for both warm and cold water; ocean currents; waves; hurricanes; seabed conditions for mounting; seabed conditions for power cables of floating plants; current local power source; annual consumption; present cost per unit; local oil or coal production; scope for other renewables; aquaculture potential; potable water potential; and environmental impacts [**100**].

3.1. The thermal structure of the ocean

Below the ocean surface, as the depth increases, the temperature of the water generally decreases [**8,21**]. The depth at which the temperature gradient, which is the rate of decrease of temperature with increase of depth, is a maximum is called the *thermocline* [**101**]. Below the water surface, the water is usually divided into three zones based on the temperature structure of the ocean: an upper zone with a depth of approximately 50 to 200 m with temperatures similar to that of the surface, a zone below 200 m and extending upto 1000 m in which the temperature changes rapidly (this is the thermocline), and a zone below 1000 m in which the temperature changes are small [**56**]. The actual depth of the zones is difficult to determine because of the minor irregularities in the temperature against depth profile. Figure 8 shows the temperature vs. depth profile at different latitudes. Figure 9 shows the temperature vs. depth profiles for some countries.

In low and middle latitudes, there is a permanent thermocline present at all the times whereas there is no permanent thermocline in polar waters [**17**]. The thermocline is shallow in spring and summer, deep in the autumn, and disappears in winter. In winter, the heat loss at the surface produces instability and the resulting convection mixes the water column to a greater depth, thus eliminating the thermocline. In the tropics, winter cooling is not strong enough to destroy the thermocline, and thus, the tropical thermocline or permanent thermocline is maintained throughout the year [**104**]. The temperature in the lower half of all the oceans is uniformly cold, with temperatures as low as 2.3ºC [**12**]. The surface temperature of the oceans range from as high as 28 ºC from the equator to -2 ºC at high latitudes. Figure 11 shows the ocean surface temperature variation with latitudes. The temperature is highest at low latitudes and decreases at higher latitudes [**56**]. In lower latitudes there is a radiation surplus (Figure 7) which decreases with increasing latitude [**52**]. It is the almost constant temperature at the beginning and end of the thermocline that can be used to drive OTEC plants. Above the thermocline, there is an almost constant source of heat and below the thermocline there is an almost constant heat sink [**22**]. An OTEC plant, which is similar to a heat engine governed by the first law of thermodynamics, is driven between the heat source and sink to produce work output [**35**], shown by a schematic diagram in Figure 10.

The temperature of the ocean water can be described in two ways: in terms of *in situ temperature* and in terms of *potential temperature* [**12**]. In situ temperature is the observed temperature of a parcel of water at a *certain depth*, whereas potential temperature is defined as the temperature of a parcel of water at the *sea surface* if it is raised adiabatically from some depth in the ocean. Adiabatically raising the parcel of water means that it is raised in an insulated container so that there is no exchange of heat with its surroundings [**105**]. The water parcel, however, is not actually brought to the surface. The potential temperature is therefore always less than the in situ temperature [**12, 105-107**]. Potential temperature finds applications for stratified fluids, which are fluids with varying densities along the axis of gravity. Changes in pressure affect the water temperature and the water temperature can increase with depth in very deep ocean

trenches and within the ocean mixed layer. The use of potential temperature eliminates these unstable conditions [**108**].

Thermal energy in the oceans is distributed by three processes, advection, diffusion, and vertical mixing. All these processes do not change the energy content of the ocean. Vertical mixing redistributes thermal energy within a column of the ocean whereas advection and diffusion move it horizontally as well [**109**]. The strength of the vertical mixing depends on the wind speeds on the ocean surface [**110**]. In a vertical water column in the ocean, the yearly changes in heat content are more notable in the upper layers of the ocean than the lowermost layers [**111**]. A vertical column of the ocean gains thermal energy from the incoming solar radiation and loses it by back radiation and evaporation. The rate of sensible heat gain or loss depends on whether the sea is warmer or colder than the air close to the ocean surface [**112**]. The vertical heat transfer can be thought of as being caused by very slow large-scale vertical water motion and by faster vertical motion in small eddies. Upwelling and downwelling can be considered as large-scale water motion, where upwelling reduces the energy content of the column because it brings up cold water from the bottom of the ocean, and downwelling increases the heat content [**111**].

The heat source and the heat sink at the beginning and end of thermocline can be used to drive OTEC plants. The analyses of basic OTEC systems are presented in sections 3.2, 3.3, and 3.4. The equations are derived from references [**22,44,87,89-91,96,97, 113,114,117**].

3.2. Closed cycle OTEC system

The analysis of the three systems is similar with most of the equations being same, since all the three systems undergo the same thermodynamic cycles. Figure 12 shows a schematic of a closed cycle OTEC system and its T-S diagram.

The net power, $\dot{W}_N$, of an OTEC plant is the net power of the thermal cycle minus the pumping power required by the working fluid pump, and the warm and cold water pumps [**22**], given as:

$$\dot{W}_N = \dot{W}_G - (\dot{W}_{WSP} + \dot{W}_{CSP} + \dot{W}_{WFP}) \tag{17}$$

where $\dot{W}_G$ is the power available at the generator, $\dot{W}_{WSP}$ is the power required for pumping warm surface water, $\dot{W}_{CSP}$ is the power required for pumping deep cold seawater, and $\dot{W}_{WFP}$ is the working fluid pumping power.

a) Generator power, $\dot{W}_G$

Since the working fluid pump, the evaporator, the condenser, and the turbine are steady flow devices, the processes of the power cycle are analyzed as steady flow processes. Work is done by the turbine, therefore positive work output. Process 1-2 is adiabatic and undergoes isentropic expansion. The generator power is given as: `

$$\dot{W}_G = \dot{m}_{WF}\eta_T\eta_G(h_1 - h_2) \tag{18}$$

where $\dot{m}_{WF}$ is the mass flowrate of working fluid, η_T is the turbine efficiency, and η_G is the generator efficiency.

b) Condenser

i) Heat rejection from working fluid in the condenser is:

$$\dot{Q}_C = \dot{m}_{WF}(h_2 - h_3) \tag{19}$$

ii) The heat gained by cold water in the condenser

$$\dot{Q}_C = \dot{m}_{CS} C_p (T_{cso} - T_{csi}) \tag{20}$$

where $\dot{m}_{CS}$ is the mass flowrate of the deep cold sea water, C_p is the specific heat, T_{cso} is the temperature of cold seawater at exit of condenser, and T_{csi} is the cold sea water temperature at inlet of condenser.

iii) The heat transfer in the condenser based on the heat transfer coefficient and the log mean temperature difference is:

$$\dot{Q}_C = U_C A_C (\Delta T_m)_C \tag{21}$$

where U_C is the overall heat transfer coefficient of the condenser, A_C is the heat transfer area of the condenser, and $(\Delta T_m)_C$ is the log mean temperature difference (LMTD) of the condenser.

The log mean temperature difference is calculated as:

$$(\Delta T_m)_C = \frac{(T_2 - T_{csi}) - (T_3 - T_{cso})}{\ln\left\{\dfrac{T_2 - T_{csi}}{T_3 - T_{cso}}\right\}} \tag{22}$$

where T_2 and T_3 are temperatures of the working fluid at the inlet and outlet of the condenser.

c) Working fluid pump power, $\dot{W}_{WFP}$

Work is done on the pump, therefore negative work output. Process 3-4 is adiabatic and undergoes isentropic compression. The working fluid pump power is calculated as:

$$\dot{W}_{WFP} = \frac{\dot{m}_{WF}(h_4 - h_3)}{\eta_{WFP}} \tag{23}$$

where η_{WFP} is the working fluid pump efficiency.

The shaft work for a steady flow device (pump) is:

$$W = \int_3^4 v.dp \tag{24}$$

The working fluid pumping power is also given as:

$$\dot{W}_{WFP} = \dot{m}_{WF} v_f (P_4 - P_3) \tag{25}$$

where v_f is the specific volume of the working fluid, and P_3 and P_4 are operating pressures.

d) Evaporator

i) Heat absorption by the working fluid in the evaporator is given as:

$$\dot{Q}_E = \dot{m}_{WF}(h_4 - h_1) \tag{26}$$

ii) The heat lost by warm water in the evaporator

$$\dot{Q}_E = \dot{m}_{WS} C_p (T_{wsi} - T_{wso}) \tag{27}$$

where $\dot{m}_{WS}$ is the mass flowrate of the warm surface sea water, C_p is the specific heat, T_{WSi} is the temperature of warm seawater at inlet of evaporator, and T_{WSO} is the warm sea water temperature at outlet of evaporator.

iii) The heat transfer in the evaporator based on the heat transfer coefficient and the log mean temperature difference is:

$$\dot{Q}_E = U_E A_E (\Delta T_m)_E \tag{28}$$

where U_E is the overall heat transfer coefficient of the condenser, A_E is the heat transfer area of the condenser, and $(\Delta T_m)_E$ is the log mean temperature difference (LMTD) of the evaporator.

The log mean temperature difference is calculated as:

$$(\Delta T_m)_E = \frac{(T_{wsi} - T_1) - (T_{wso} - T_4)}{\ln\left\{\dfrac{T_{wsi} - T_1}{T_{wso} - T_4}\right\}} \tag{29}$$

where T_1 and T_4 are temperatures of the working fluid at the inlet and outlet of the evaporator.

e) Cold sea water pumping power, $\dot{W}_{CSP}$

The cold seawater pumping power is given as:

$$\dot{W}_{CSP} = \frac{\dot{m}_{CS}\, g \Delta h_{CSP}}{\eta_{CSP}} \tag{30}$$

where η_{CSP} is the pump efficiency, g is the gravitational acceleration, and Δh_{CSP} is the total head loss in the cold water pipe. The total head loss across the cold water piping system is:

$$\Delta h_{CSP} = (\Delta h_{CS})_{SP} + (\Delta h_{CS})_M + (\Delta h_{CS})_C + (\Delta h_{CS})_d \quad (31)$$

where $(\Delta h_{CS})_{SP}$, is the head loss due to friction in the straight pipe, $(\Delta h_{CS})_M$ is the minor head losses due to bends, $(\Delta h_{CS})_C$ is head loss of cold water in the condenser, and $(\Delta h_{CS})_d$ is the head loss due to density differences. The cold seawater pumping power is thus given as:

$$\dot{W}_{CSP} = \frac{\dot{m}_{CS} g\left[(\Delta h_{CS})_{SP} + (\Delta h_{CS})_M + (\Delta h_{CS})_C + (\Delta h_{CS})_d\right]}{\eta_{CSP}} \quad (32)$$

e) Warm sea water pumping power, $\dot{W}_{WSP}$

The warm surface seawater pumping power is given as:

$$\dot{W}_{WSP} = \frac{\dot{m}_{WS} g \Delta h_{WSP}}{\eta_{WSP}} \quad (33)$$

where η_{WSP} is the pump efficiency, g is the gravitational acceleration, and Δh_{WSP} is the total head loss in the warm water pipe. The total head loss across the warm water piping system is:

$$\Delta h_{WSP} = (\Delta h_{WS})_{SP} + (\Delta h_{WS})_M + (\Delta h_{WS})_E \quad (34)$$

where $(\Delta h_{WS})_{SP}$, is the frictional headloss in the straight pipe, $(\Delta h_{WS})_M$ is the minor head losses in the pipe due to bends, and $(\Delta h_{WS})_E$, is the head loss of warm water in the evaporator. The warm seawater pumping power is thus given as:

$$\dot{W}_{WSP} = \frac{\dot{m}_{WS} g\left[(\Delta h_{WS})_{SP} + (\Delta h_{WS})_M + (\Delta h_{WS})_E\right]}{\eta_{WSP}} \quad (35)$$

3.3. Open cycle OTEC system

Figure 13 shows a schematic of an open cycle OTEC system and its T-S diagram.

The net power, $\dot{W}_N$, is given as:

$$\dot{W}_N = \dot{W}_G - (\dot{W}_{WSP} + \dot{W}_{CSP} + \dot{W}_V) \tag{36}$$

where $\dot{W}_G$ is the power available at the generator, $\dot{W}_{WSP}$ is the power required for pumping warm surface water, $\dot{W}_{CSP}$ is the power required for pumping deep cold seawater, and $\dot{W}_V$ is the power required by the vacuum pump.

a) Generator power, $\dot{W}_G$

The generator power is calculated as:

$$\dot{W}_G = \eta_T \dot{Q}_{in} \left(1 - \frac{(T_{steam})_{cond}}{T_{wsi}} \right) \tag{37}$$

where η_T is the turbine efficiency, $\dot{Q}_{in}$ is the heat input to the system, T_{wsi} is the temperature of warm seawater entering the flash evaporator, and $(T_{steam})_{cond}$ is the condensing temperature of steam.

b) Heat transfer in the condenser when steam condenses:

$$\dot{Q}_C = \dot{m}_{steam}(h_3 - h_5) \tag{38}$$

where $\dot{m}_{steam}$ is the mass flowrate of steam, h_3 is the enthalpy of vapor before the turbine, and h_5 is the enthalpy of vapor at exit of turbine. The mass flowrate of steam is calculated as:

$$\dot{m}_{steam} = \frac{\dot{m}_{ws} C_p (T_{wsi} - T_{wso})}{H_{fg} - C_p (T_{wso} - T_{sat})} \tag{39}$$

where $\dot{m}_{ws}$ is the mass flowrate of warm surface water, C_p is the specific heat, T_{wsi} is the warm water temperature at inlet of flash evaporator, T_{wso} is the warm water temperature at exit of flash evaporator, H_{fg} is the latent heat of vaporization, and T_{sat} is the saturation temperature at corresponding flash evaporator pressure.

ii) the heat gained by cold water in the condenser is given by equation 20:

$$\dot{Q}_C = \dot{m}_{CS} C_p (T_{cso} - T_{csi})$$

where $\dot{m}_{CS}$ is the mass flowrate of the deep cold sea water, C_p is the specific heat, T_{cso} is the temperature of cold seawater at exit of condenser, and T_{csi} is the cold sea water temperature at inlet of condenser.

iii) The heat transfer in the condenser based on the heat transfer coefficient and the log mean temperature difference is given by equation 22:

$$\dot{Q}_C = U_C A_C (\Delta T_m)_C$$

where U_C is the overall heat transfer coefficient of the condenser, A_C is the heat transfer area of the condenser, and $(\Delta T_m)_C$ is the log mean temperature difference (LMTD) of the condenser

c) Heat transfer in the flash evaporator is given by equation 27:

$$\dot{Q}_{FE} = \dot{m}_{WS} C_P (T_{WSi} - T_{WSO})$$

where $\dot{m}_{WS}$ is the mass flowrate of the warm surface sea water, C_p is the specific heat, T_{WSi} is the temperature of warm seawater at inlet of flash evaporator, and T_{WSO} is the warm sea water temperature at outlet of flash evaporator.

Cold water pumping power

e) Cold sea water pumping power, $\dot{W}_{CSP}$

The cold seawater pumping power is given by equation 30:

$$\dot{W}_{CSP} = \frac{\dot{m}_{CS} g \Delta h_{CSP}}{\eta_{CSP}}$$

where η_{CSP} is the pump efficiency, g is the gravitational acceleration, and Δh_{CSP} is the total head loss in the cold water pipe. The total head loss across the cold water piping system is:

$$\Delta h_{CSP} = (\Delta h_{CS})_{SP} + (\Delta h_{CS})_M + (\Delta h_{CS})_C + (\Delta h_{CS})_d \quad (40)$$

where $(\Delta h_{CS})_{SP}$ is the head loss due to friction in the straight pipe, $(\Delta h_{CS})_M$ is the minor head losses due to bends, $(\Delta h_{CS})_C$ is head loss of cold water in the condenser, and $(\Delta h_{CS})_d$ is the head loss due to density differences. The cold seawater pumping power is thus given as:

$$\dot{W}_{CSP} = \frac{\dot{m}_{CS} g\left[(\Delta h_{CS})_{SP} + (\Delta h_{CS})_M + (\Delta h_{CS})_C + (\Delta h_{CS})_d\right]}{\eta_{CSP}} \quad (41)$$

Warm water pumping power

e) Warm sea water pumping power, $\dot{W}_{WSP}$

The warm surface seawater pumping power is given by equation 33:

$$\dot{W}_{WSP} = \frac{\dot{m}_{WS} g \Delta h_{WSP}}{\eta_{WSP}}$$

where η_{WSP} is the pump efficiency, g is the gravitational acceleration, and Δh_{WSP} is the total head loss in the warm water pipe. The total head loss across the warm water piping system is: The total head loss across the cold water piping system is:

$$\Delta h_{WSP} = (\Delta h_{WS})_{SP} + (\Delta h_{WS})_{M} + (\Delta h_{WS})_{FE} \tag{42}$$

where $(\Delta h_{WS})_{SP}$, is the frictional headloss in the straight pipe, $(\Delta h_{WS})_{M}$ is the minor head losses in the pipe due to bends, and $(\Delta h_{WS})_{FE}$ is the head loss across the flash evaporator. The warm seawater pumping power is thus given as:

$$\dot{W}_{WSP} = \frac{\dot{m}_{WS} g\left[(\Delta h_{WS})_{SP} + (\Delta h_{WS})_{M} + (\Delta h_{WS})_{FE}\right]}{\eta_{WSP}} \tag{43}$$

3.4. Hybrid cycle OTEC system

Figure 14 shows a schematic of a hybrid cycle OTEC system and its T-S diagram.

The net power, $\dot{W}_N$, is given as:

$$\dot{W}_N = \dot{W}_G - (\dot{W}_{WSP} + \dot{W}_{CSP} + \dot{W}_{WFP} + \dot{W}_V) \tag{44}$$

Where $\dot{W}_G$ is the power available at the generator, $\dot{W}_{WSP}$ is the power required for pumping warm surface water, $\dot{W}_{CSP}$ is the power required for pumping deep cold seawater, $\dot{W}_{WFP}$ is the working fluid pumping power, and $\dot{W}_V$ is the power required by the vacuum pump.

Power cycle analysis

a) Generator power, $\dot{W}_G$

The generator power is calculated using equation 18:

$$\dot{W}_G = \dot{m}_{WF}\eta_T\eta_G(h_1 - h_2)$$

where $\dot{m}_{WF}$ is the mass flowrate of the working fluid, η_T is the turbine efficiency, and η_G is the generator efficiency.

b) Condenser

i) The heat rejection from the working fluid in the condenser is calculated using equation 19:

$$\dot{Q}_C = \dot{m}_{WF}(h_2 - h_3)$$

ii) Heat gained by cold water in the condenser is calculated using equation 20:

$$\dot{Q}_C = \dot{m}_{CS}C_p(T_{cso} - T_{csi})$$

iii) The heat transfer in the condenser based on the heat transfer coefficient and the log mean temperature difference is calculated using equation 22:

$$\dot{Q}_C = U_C A_C(\Delta T_m)_C$$

c) Working fluid pump power, $\dot{W}_{WFP}$

The working fluid pumping power is given by equations 23 and 25:

$$\dot{W}_{WFP} = \frac{\dot{m}_{WF}(h_4 - h_3)}{\eta_{WFP}}$$

$$\dot{W}_{WFP} = \dot{m}_{WF} v_f (P_4 - P_3)$$

d) Evaporator

i) Heat absorption by the working fluid in the evaporator is given by equation 26:

$$\dot{Q}_E = \dot{m}_{WF}(h_4 - h_1)$$

ii) The heat lost by warm water in the evaporator is given by equation 27:

$$\dot{Q}_E = \dot{m}_{WS} C_p (T_{wsi} - T_{wso})$$

iii) The heat transfer in the evaporator based on the heat transfer coefficient and the log mean temperature difference is calculated using equation 28:

$$\dot{Q}_E = U_E A_E (\Delta T_m)_E$$

Cold water pumping power

e) Cold sea water pumping power, $\dot{W}_{CSP}$

The cold seawater pumping power is given by equation 30:

$$\dot{W}_{CSP} = \frac{\dot{m}_{CS} g \Delta h_{CSP}}{\eta_{CSP}}$$

The total head loss across the cold water piping system is:

$$\Delta h_{CSP} = (\Delta h_{CS})_{SP} + (\Delta h_{CS})_M + (\Delta h_{CS})_C + (\Delta h_{CS})_d + (\Delta h_{CS})_{DC} \quad (45)$$

where $(\Delta h_{CS})_{SP}$ is the head loss due to friction in the straight pipe, $(\Delta h_{CS})_M$ is the minor head losses due to bends, $(\Delta h_{CS})_C$ is head loss of cold water in the condenser, $(\Delta h_{CS})_d$ is the head loss due to density differences and $(\Delta h_{CS})_{DC}$ is the head loss in the desalination condenser. The cold seawater pumping power is thus given as:

$$\dot{W}_{CSP} = \frac{\dot{m}_{CS} g\left[(\Delta h_{CS})_{SP} + (\Delta h_{CS})_M + (\Delta h_{CS})_C + (\Delta h_{CS})_d + (\Delta h_{CS})_{DC}\right]}{\eta_{CSP}} \quad (46)$$

Warm water pumping power

e) Warm sea water pumping power, $\dot{W}_{WSP}$

The warm surface seawater pumping power is given by equation 33:

$$\dot{W}_{WSP} = \frac{\dot{m}_{WS} g \Delta h_{WSP}}{\eta_{WSP}}$$

The total head loss across the cold water piping system is:

$$\Delta h_{WSP} = (\Delta h_{WS})_{SP} + (\Delta h_{WS})_M + (\Delta h_{WS})_E + (\Delta h_{WS})_{fc} \quad (47)$$

where $(\Delta h_{WS})_{SP}$, is the frictional headloss in the straight pipe, $(\Delta h_{WS})_M$ is the minor head losses in the pipe due to bends, $(\Delta h_{WS})_E$ is the head loss of warm water in the evaporator, and $(\Delta h_{WS})_{fc}$ is the head loss across the flash chamber. The warm seawater pumping power is thus given as:

$$\dot{W}_{WSP} = \frac{\dot{m}_{WS} g \left[(\Delta h_{WS})_{SP} + (\Delta h_{WS})_{M} + (\Delta h_{WS})_{E} + (\Delta h_{WS})_{fc} \right]}{\eta_{WSP}} \quad (48)$$

3.5. Feasibility, technological issues, and impacts of OTEC plants

Ocean thermal energy conversion plants can be located across about 60 million square kilometers of tropical oceans, generally at latitudes within about 20 or 25 degrees of the equator. Ocean water more than 1000 meters below the surface is normally at a temperature of about 4 ºC. This vast resource of cold water is constantly supplied by the deep cold water that flows from the polar regions [**22,119**].

3.5.1 Feasibility

There is a high potential for OTEC plants in tropical island countries where the temperature difference between surface and deep cold water at 1000 m is approximately between 20 - 24ºC and is sufficient to operate OTEC plants [**22**]. The ocean thermal gradient essential for OTEC plants operation is mostly found between latitudes 20ºN and 20ºS [**120,121**]. There are at least two separate markets for OTEC plants: (i) industrial nations and islands, (ii) smaller or less industrialized islands with modest needs for power as well as desalinated water [**122**].

Commercial OTEC plants should be located in a stable resourceful environment for efficient operation of the system [**123**]. The country's population, economies, policies and energy demands should also be looked at. An energy analysis that involves the environment, economy, and services should be put together for an emergy evaluation (emergy with an 'm') to determine the cost benefits [**124**]. Since capital costs are very high for OTEC plants, the by-products of these plants, such as fresh water, should be considered in a financing strategy to help overcome the initial costs [**125**]. Studies have been done by Srinivasan et al. [**126**] on the cost effectiveness of OTEC plants and they designed a new OTEC system by introducing a subsea condenser. When identifying

locations for OTEC plants, the thermal gradient suitable to drive the plants should not be very far away from the shore. The OTEC piping systems are a major part of the initial capital cost of OTEC plants [**119**]. Table 1 shows some countries with their thermal gradients and the distance of the thermal resource from the shore.

Ocean thermal energy conversion plants can be land based, shelf mounted on platforms, or floating types on deep water [**127,128**]. The plants installed on or near land do not require complicated mooring, long power cables, or high maintenance costs such as with open-ocean environments. They can be installed in sheltered areas to keep it safe from storms and heavy seas. Land based or near shore located OTEC plants can be operated in combination with industries such as for mariculture or for desalinated water [**127,129**]. A shelf mounted OTEC plant can be towed to a favorable site of about 100 m depth and fixed to the sea bottom. This is done to have closer access to the cold water resource. Shelf mounted plants has to bear the open ocean environmental conditions and the power delivery is also a concern because of the long underwater cables required to reach land [**127,129**]. Floating OTEC plants are designed to operate offshore, and are preferred for large power capacity plants. Offshore plants are difficult to stabilize and to moor in deep water, and the cables attached to floating plants are more vulnerable to damages in the open ocean environments. External forces such as waves, wind, and ocean currents affect the stability of the plant [**127,130**].

3.5.1.1 Some OTEC case studies

The first ever OTEC plant that was successfully commissioned was in Hawaii in 1979. A 50 kW closed cycle floating demonstration plant was constructed offshore. Cold water at a temperature of 4.4 °C was drawn from a depth of 670 m. The seabed at the site was a steep rocky volcanic slope with very rough topography. The platform was moored by using a 30000 lb submerged weight. Ammonia was used as the working fluid. Polyethylene pipe was used for transporting cold water. Polyethylene has a very smooth interior and this reduces biofouling [**131**]. Two plate type titanium heat exchangers were used [**132**]. During actual operation of the plant, it was found that biofouling, effects of

mixing the deep cold water with the warm surface water, and debris clogging did not have any negative effects on plant operation. The longest continuous operation was for 120 hours. The plant designers had expected 50 kW of electricity to be generated and 40 kW to be consumed in running the pumps and other equipment on board, and these were met [**131**].

A 100 kW OTEC pilot plant was constructed on-land for demonstration purposes in the republic of Nauru in October 1981 by Japan. This pilot plant proved the validity of the mechanical and electrical designs and also the deepwater pipelines for deep cold water. The system operated between the warm surface water and the cold heat source of 5-8°C at a depth of 500-700 m, with a temperature difference of 20°C. A pipeline length of 945 m was required to reach a depth of 580 m. Freon-22 was used as the working fluid in the closed cycle because it is less harmful compared to ammonia. The heat exchanger tubes were surface treated with titanium to improve performance. The shape of the seabed was very irregular from the lagoon tip to a 50 m depth, after which there was a continuous slope with a 40-45 degree inclination. This favorable coastal site was utilized to construct the demonstration plant on land. The pipe material used was polyethylene after investigating the thermal and mechanical stresses. Polyethylene pipes are superior in flexibility to steel pipes and adapts well to seabed irregularity [**133**]. The tests done were load response characteristics, turbine, and heat exchanger performance tests. The internal efficiency of the turbine was well over 80%. Heat exchanger performance was highly satisfactory. During operation, warm water from the surface brought some seaweeds and sand, but nothing was trapped in the screen for cold water. The plant had operated by two shifts with one spare shift, and a continuous power generation record of ten days was achieved. The plant produced 31.5 kW of OTEC net power during continuous operation and was connected to the main power system [**133**].

A 1 MW floating demonstration plant was planned to be built off the coast of Tamil Nadu by the National Institute of Ocean Technology (NIOT), India, with a gross power generation capacity of 1MW and a net power 500 kW. This was to be commissioned south east of Tutricorin, South India. The plant was supposed to have ammonia as a

working fluid and would have been the world's first floating plant. The evaporators had a special steel coating on the ammonia side to enhance nucleate boiling. An after-condenser was introduced after laboratory tests. A four stage ammonia turbine was also developed and the plant was integrated on a floating barge. The floating barge was to be moored on a single point mooring at a depth of 1200 m using a 1 m diameter high density Poly Ethylene pipe, which was the intake for the cold water pipe [**94**]. Even though all the components were tested before commissioning, there was a problem in establishing the 1 km long high density Polyethylene pipeline. Thus, this project was abandoned with focus diverted to desalination using the OTEC cold water pipe [**134**].

A land based open cycle OTEC experimental plant was installed in Hawaii in 1993. The turbine-generator was designed for an output of 210 kW for 26°C warm surface water and 6°C deep water temperature. A small fraction (10 percent) of the steam produced was condensed using a surface condenser to produce desalinated water. The experimental plant successfully operated for six years. The highest gross power achieved was 255 kWe with a corresponding net power of 103 kW and 0.4 L/s of desalinated water [**30**].

Saga University, Japan, is actively involved in OTEC and its byproduct studies. Experimental studies have been conducted on heat exchangers for use as evaporators and condensers. A spray-flash evaporation desalination system is also being investigated. This desalination system can be utilized to convert 1% of raw seawater to fresh water. Other studies done are on mineral water production using deep cold water, lithium extraction from seawater, hydrogen production, air-conditioning and aquaculture applications using deep cold water, and using the deep cold water for food processing and medical (cosmetic) applications [**135**].

3.5.2 Technological issues

The proper designs of OTEC systems include the consideration of leakage of piping systems that carry ammonia in a closed cycle. A major disadvantage of OTEC systems is the high capital cost [**79**]. Extensive research has been done on the OTEC components,

for example, heat exchangers should have compact designs with optimum heat transfer and low unit cost [**136**]. Experimental studies on heat exchangers for use in OTEC plants have also been conducted in Saga University, Japan [**22**]. Guo-Yan et al. [**137**] has presented a techno-economic study on compact heat exchangers to choose an optimum heat exchanger with minimum pressure drop. They concluded that all compact heat exchangers are feasible from an energetic point of view. However the performance differs due to the materials used. Biofouling in the heat exchangers provides resistance to heat transfer, therefore affecting their performance [**87**]. Cleaning methods such as continual circulation of close fitting balls and by chemical additives to the water are used [**87**]. Together with a large pressure difference across the turbine, a high heat transfer rate between the working fluid and the ocean water in the heat exchangers is required for optimal power production in OTEC plants. Very large size turbines are required for the low temperature and low pressure vapor at the evaporator [**22**].

Another major design concern is the cold water pipe that transports cold water from the deep ocean to the surface. The cold water pipes that pump deep cold ocean water to the surface require a lot of pumping power which increases the costs [**113**]. Approximately 4 m^3/s of warm surface seawater and 2 m^3/s of deep cold seawater (ratio 2:1), for a temperature difference of 20ºC, are required for every MW of electricity generated [**138**]. It is subjected to forces such as drag by ocean currents, oscillation forces, stresses at the connections, forces due to harmonic motion of the platform, ad the dead weight of the pipe itself. Also, problems will arise during installation due to difficulties in construction and transportation to deployment site due to its very large size. The choice of materials is also debatable [**22,87, 139**]. The successful installations of offshore oil drilling platforms have provided technical guidance that can be directly applicable to OTEC cold water pipe design [**22**].

3.5.3 Environmental impacts of OTEC plants

Renewable energy utilization will always have some impacts on the environment. Ocean thermal energy conversion plants will have an impact on the physical characteristics of

the region it is deployed in [**140**]. These plants can be used to help improve the environment by combining it with artificial coral reef ecosystems [**141**]. However, changes in the climate characteristics are also possible [**140**]. Ocean thermal energy conversion plants can alter the ocean surface energy balance by lowering the surface temperatures, the tropical ocean environment can be modified by OTEC implemented upwelling and increase in CO_2 production due to increased mixing rate between surface and deep ocean waters. The deep water temperature can increase and the albedo of the surface can also increase due to increased phytoplankton on the surface [**22,140**].

Deep cold seawater used in OTEC plants contains a lot of dissolved inorganic nutrients such as phosphate, nitrate and silicate, which could be expected to promote blooms of photosynthetic organisms if the seawater is discharged and contained within the upper ocean or in coastal waters [**142**]. However, the rich nutrients will be discharged at the surface which is poor in nutrients and is much warmer compared to deep ocean water. The resulting complications due to this forced nutrient mixing are not fully understood [**143**]. Alterations in climate and ocean surface conditions will be more significant when multiple OTEC plants operate in a region. Also, the water intake by OTEC plants at the ocean surface would induce circulation, which could affect the coastal circulation [**22**]. An experimental an analytical study conducted by Jirka et al. [**144**] on the mixing and recirculation of surrounding ocean waters of an OTEC plant shows that large discharge velocities and plant flowrates contribute a lot to recirculation.

4. CONCLUSIONS

The heat exchange processes across the ocean surface and the technology for ocean thermal energy conversion are presented. The heat exchange processes across the ocean surface are represented in an ocean energy budget. The heat added to the ocean by short wave radiation is different at different latitudes and over different seasons, the maximum being at the equator. Heat lost by back radiation from the surface of the ocean increases with decreasing altitudes of the Sun. The effective back radiation from the ocean surface is the difference between the outward radiation from the surface and the re-radiation (or

down radiation) from the atmosphere. Heat lost by evaporation from the ocean surface is the largest contributing factor to the overall heat losses from the ocean. The evaporation is higher close to the equator and decreases with increasing latitudes. Heat lost by convection and conduction has seasonal and regional variations, and depends on the temperature difference between the ocean surface and the air close to the surface. Ocean currents transfer thermal energy from the lower latitudes to cooler regions in the higher latitudes. The ocean energy budget quantifies the amount of heat gained and lost by the ocean, and this can be used to determine the overall temperature change of the system over a certain period of time. The accurate measurements and predictions of the ocean energy budget terms are difficult and some errors and imbalances are still present. The transport of cold water from the higher latitudes towards the equator along the ocean bottom results in the displacement of the lower density water above and creates a thermal structure with a large reservoir of warm water at the ocean surface and a large reservoir of cold water at the bottom, with a temperature difference between them of 22ºC to 25ºC. This temperature difference can be used to drive an ocean thermal energy system. Ocean thermal energy conversion (OTEC) plants operate using this temperature difference to run a turbine with efficiencies close to 3%. The thermal structure of the oceans, or the thermocline, varies with different latitudes and is permanent for lower latitudes. The thermodynamic principles are similar for the basic cycles, namely, open cycle, closed cycle, and hybrid cycle. There are many technological issues for OTEC plant implementation, such as getting cold water from the ocean depths, which is a major concern. Many technological problems are however solved, such as fouling and compact designs of heat exchangers. The case studies clearly show that OTEC technology can be successfully commissioned. However, proper design and planning is required. It is seen that most of the power generated at the turbine is used up in running the pumps and other equipment. The first 50 kW OTEC plant in Hawaii in 1979 used 40 kW of the power in running the pumps and other equipment on board. The initial capital cost for OTEC plants is very large, but once the plant is operational, the costs will be recovered in the long run. Ocean thermal energy conversion plants can alter the ocean surface energy balance by altering the surface temperatures and increased CO_2 production due to

increased mixing of surface and deep waters. But no such issues were faced during the actual operation of the demonstration OTEC plants in Hawaii and Nauru.

NOMENCLATURE

A_C = Heat transfer area of condenser, m^2

Ae = Eddy diffusivity of water vapor, m^2/s

A_E = Heat transfer area of evaporator, m^2

A_h = Eddy conductivity, kg/m.s

A_n = Noon altitude of the sun, Degrees

B = Bowen's Ratio

C = Cloud cover, Okta

C_p = Specific heat of air (or water) at constant pressure, kJ/kg.ºC

dt/dz = Vertical temperature gradient in the lowest atmosphere, ºC/m

de/dz = Gradient of water vapor concentration in the air above ocean surface

e_a = Actual vapor pressure at 10 m above ocean surface, kPa

e_s = Saturated water vapor pressure at ocean surface, kPa

F_e = Rate of evaporation of water**,** kg/s per square meter of sea surface

g = Gravitational acceleration, m/s^2

h = Enthalpies, kJ/kg

H_{fg} = Latent heat of vaporization, kJ/kg

L_t = Latent heat of vaporization, kJ/kg

$\dot{m}_{CS}$ = Mass flowrate of cold seawater, m^3/s

$\dot{m}_{Steam}$ = Mass flowrate of steam, m^3/s

$\dot{m}_{WF}$ = Mass flowrate of working fluid, m^3/s

$\dot{m}_{WS}$ = Mass flowrate of warm seawater, m^3/s

N = Precipitation, cm/year

P = Operating pressures, Pa

$\dot{Q}_b$ =Rate of heat loss from the ocean by back radiation, W/m^2

$\dot{Q}_C$ = Heat transferred in the OTEC condenser, W

$\dot{Q}_E$ = Heat transferred in the OTEC evaporator, W

$\dot{Q}_e$ = Rate of heat loss by evaporation from the ocean surface, W/m^2

$\dot{Q}_h$ = Rate of sensible heat loss from ocean surface by convection and conduction,W/m^2

$\dot{Q}_r$ = Amount of short-wave radiation reflected from the ocean surface, W/m^2

$\dot{Q}_S$ =Rate of heat added to ocean by short-wave solar radiation, W/m^2

$\dot{Q}_S$' = Amount of solar radiation received by ocean surface after cloud disturbance approximations, W/m^2

$\dot{Q}_T$ = Total rate of heat gain or loss by a given area of the ocean, W/m^2

$\dot{Q}_V$ = Heat transported by moving currents (advection) within the ocean, W/m^2

S = Salinity, parts per thousand $\left(\frac{o}{oo}\right)$

t = Period, s

T = Temperature, ºC

T_a = Air temperature at standard height (10 m) above ocean surface, ºC

t_d = Length of day (sunrise to sunset), hours

T_s = Ocean surface temperature, ºC

T_{wsi} = Warm seawater temperature at inlet of evaporator, ºC

T_{WSO} = Warm seawater temperature at outlet of evaporator, ºC

T_{CSi} = Cold seawater temperature at inlet of condenser, ºC

T_{CSO} = Cold seawater at outlet of condenser, ºC

$(T_{steam})_{cond}$ = Temperature of steam in open cycle OTEC condenser, ºC

U_C = Overall heat transfer coefficient of condenser, W/m^2.K

U_E = Overall heat transfer coefficient of evaporator, W/m^2.K

V = Evaporation, cm/year

v_f = Specific volume of liquid working fluid, m^3/kg

W = Wind speed at 10 m above sea surface, m/s

$\dot{W}_G$ = Generator power of an OTEC plant, W

$\dot{W}_N$ = Net power of an OTEC plant, W

$\dot{W}_V$ = Vacuum pump power, W

$\dot{W}_{CSP}$ = Power required by cold seawater pump, W

$\dot{W}_{WSP}$ = Power required by warm seawater pump, W

$\dot{W}_{WFP}$ = Power required by working fluid pump, W

η_G = Efficiency of generator

η_T = Efficiency of turbine

η_{CSP} = Efficiency of cold seawater pump

η_{WFP} = Efficiency of working fluid pump

η_{WSP} = Efficiency of warm seawater pump

Δh_{CSP} = Total head loss across cold water piping, m

Δh_{WSP} = Total head loss across cold water piping, m

$(\Delta h_{CS})_C$ = Head losses in the condenser, m

$(\Delta h_{WS})_E$ = Head losses in the evaporator, m

$(\Delta h_{CS})_d$ = Head losses due to density differences, m

$(\Delta h_{CS})_M$ = Minor head losses in the cold water pipe, m

$(\Delta h_{WS})_M$ = Minor head losses in the warm water pipe, m

$(\Delta h_{CS})_{DC}$ = Head loss in the desalination condenser, m

$(\Delta h_{WS})_{FE}$ = Head losses in the flash evaporator of open cycle system, m

$(\Delta h_{CS})_{SP}$ = Frictional head loss in cold water pipe, m

$(\Delta h_{WS})_{SP}$ = Frictional head loss in warm water pipe, m

$(\Delta h_{WS})_{fc}$ = Head losses in the flash chamber of hybrid cycle system, m

$(\Delta T_m)_C$ = Log mean temperature difference of condenser, ºC

$(\Delta T_m)_E$ = Log mean temperature difference of evaporator, ºC

ΔT = Change in seawater temperature, ºC

ρ = Seawater density, kg/m^3

σ = Stefan-Boltzmann constant, Wm^{-2}K^{-4}

REFERENCES

1. Hilgenkamp K. *Environmental health: ecological perspectives*. Jones & Bartlett Learning: Canada, 2006; 152.
2. *World Ocean*. Available from: http://en.wikipedia.org/wiki/World_Ocean. Accessed on: 16.03.2010.
3. Hale N. *An epitome of universal geography or, A description of the various countries of the globe: with a view of their political condition at the present time*. N Hale: Boston, 1830; 5.
4. Gross MG, Gross E. *Oceanography, a View of Earth, 7th edition*. Prentice Hall: New Jersey, 1996; 90-173.
5. Garrison T. *Essentials of oceanography, 5th edition*. Cengage Learning: USA, 2008; 126-205.
6. Webster PJ. The role of hydrological processes in ocean – atmosphere interactions. *Reviews of geophysics* 1994; 32: 427-476.
7. Garrison T. Oceanography: an invitation to marine science, 6th edition. Cengage Learning: USA, 2007; 230
8. Charles L. Drake, John Imbrie, John A. Knauss, Karl K. Turekian. *Oceanography*. Rinehart and Winston: USA, 1978; 50-73.
9. Willis JK, Roemmich D, Cornuelle B. Interannual variability in the upper ocean heat content, temperature, and thermosteric expansion on global scales. *Journal of geophysical research* 2004; 109: C12036, doi: 10.1029/2003Jc002260.
10. Coe H, Webb AR. *Atmospheric energy and structure of the atmosphere*. In: Hewitt CN, Jackson AV, editors. Handbook of atmospheric science: principles and applications. Wiley – Blackwell: USA, 2003; 35-58.
11. Tomczak M. *Regional Oceanography – an Introduction*. Pergamon: Great Britain, 1994; 2-53.
12. Knauss JA. *Introduction to Physical Oceanography*. Prentice-Hall: New Jersey, 1978; 39-134.

13. Wang W, McPhaden M. The Surface-Layer Heat Balance in the Equatorial Pacific Ocean. Part I: Mean Seasonal Cycle. *Journal of Physical Oceanography* 1999; 29: 1812 – 1831.
14. Stewart RH. *Introduction to Physical Oceanography*. Texas A & M University: Texas, 2005; 50-55.
15. *All about oceans and seas.* 2000. Available from: http://www.enchantedlearning.com/subjects/ocean/. Accessed on: 06.04.2010.
16. Emiliani C. The oceanic lithosphere. Harvard University Press: USA, 1981; 3 – 5.
17. Reddy MPM. *Descriptive Physical Oceanography*. A.A. Balkema Publishers: India, 2001; 320-329.
18. Vranes K, Gordon AL, Ffield A. The heat transport of the Indonesian Throughflow and implications for the Indian Ocean heat budget. *Deep-sea Research II* 2002; 49: 1391-1410.
19. Tolmazin D. *Elements of dynamic oceanography*. John Wiley and Sons: Cambridge, 1985; 45.
20. Walin G. On the relation between sea-surface heat flow and thermal circulation in the sea. *Tellus* 1982; 34: 187 – 195.
21. Singh S. *Geography for the Upsc civil services preliminary examination*. Tata McGraw-Hill: New Delhi, 2006; 4.11 – 4.13.
22. Avery WH, Wu C. *Renewable Energy from the Ocean - A Guide to OTEC*. Oxford University Press: Oxford, 1994; 1-367.
23. National Research Council (U.S.). Committee on Oceanography. *A review of 'Oceanography 1960-1970' and comments on the Interagency Committee on Oceanography fiscal year 1962 program*. National Academics: Washington, 1961. 10 – 14.
24. Pedlosky J. *Geophysical fluid dynamics, 2nd edition*. Springer: New York, 1987; 441 – 456.
25. Dowling TE, Showman AP. *Earth as a planet: atmosphere and oceans*. In: McFadden LA, Weissman PR, Johnson TV, editors. Encyclopedia of the solar system, 2nd edition. Academic Press: USA, 2007; 169 – 188.
26. Byrne K. *Environmental Science, 2nd edition*. Nelson Thornes: UK, 2001; 60.

27. Dincer I, Rosen MA. A worldwide perspective on energy, environment and sustainable development. International Journal of Energy Research 1998; 22: 1305-1321
28. Pelc P, Fujita RM. Renewable energy from the ocean. *Marine Policy* 2002; 26: 471-479.
29. Çengel Y. Green thermodynamics. *International Journal of Energy Research* 2007; 31:1088-1104.

30. Nihous GC, Syed MA, Vega LA. Conceptual Design of an Open Cycle OTEC Plant for the Production of Electricity and Fresh Water in a Pacific Island. In: *Proceedings of the First International Conference on Ocean Energy Recovery ICOER*, American Society of Civil Engineers, 1989.
31. Younos T, Tulou KE. Energy Needs, Consumption and Sources. *Journal of Contemporary Water Research & Education* 2005; 132: 27-38
32. Srinivasan J. *Oceans and Tropical Climate*. In: Somayajulu BLK, editor. Ocean Science – trends and Future Directions. Indian National Science Academy and Akademia Books International: India, 1999; 53-87.
33. National Renewable Energy Laboratory. *Ocean thermal energy conversion – benefits of OTEC*. Available from: http://www.nrel.gov/otec/benefits.html. Accessed on: 29.04.2010.
34. Tanner D. Ocean Thermal Energy Conversion: Current Overview and Future Outlook. *Renewable Energy* 1995; Vol. 6 No. 3: 367-373.
35. *Huang JC, Krock HJ, Oney SK. Revisit Ocean Thermal Energy Conversion System. Mitigation and Adaptation Strategies for Global Change* 2003; 8: 157-175.
36. Saur JFT, Anderson ER. The Heat Budget of a body of Water of Varying Volume. *Limnology and Oceanography* 1956; : 247-251
37. Ganachaud A. *The global oceanic heat budget*. Available from: http://www.es.flinders.edu.au/~mattom/IntroOc/notes/lecture04.html. Accessed on: 19.05.2010

38. Josey SA, Kent EC, Taylor PK. New Insights into the Ocean Heat Budget Closure Problem from the Analysis of the SOC Air-Sea Flux Climatology. *Journal of Climate* 1999; 12: 2856-2880.
39. Dera J. *Marine Physics*. PWN- Polish Scientific Publishers: Warszawa, 1992; 340-376.
40. The Open University course team. *Ocean Circulation, 2nd edition*. Butterworth-Heinemann: Oxford, 2002; 190 – 200.
41. Ochoa G, Hoffman R, Tin T. *Climate: the force that shapes our world and the future of life on earth*. Rodale Books International: London, 2005; 24 – 28.
42. Stewart RH. *Chapter 5 – The oceanic heat budget*. Available from: http://oceanworld.tamu.edu/resources/ocng_textbook/chapter05/chapter05_01.htm Accessed on: 29.04.2010.
43. Bowden KF .*Physical Oceanography of Coastal Waters*. Ellis Horwood Ltd: Chichester, 1983; 220 -222.
44. Çengel YA, Boles MA. *Thermodynamics, an engineering approach, 6th edition in SI units*. McGraw Hill: New York, 2007; 565-622.
45. Ingle (Jr), JC. *Atmosphere – Ocean coupling and surface circulation of the ocean*. In: Ernst WG, editor. Earth systems: processes and issues. Cambridge University Press: USA, 2000; 155 – 157.
46. Haney RL. Surface Thermal Boundary Condition for Ocean Circulation Models. *Journal of physical oceanography* 1971; 1: 241 – 248.
47. Swenson MS, Hansen DV. Tropical Pacific Ocean Mixed Layer Heat Budget: The Pacific Cold Tongue. *Journal of physical oceanography* 1999; 29: 69 – 81.
48. Delcroix T. Net heat gain of the tropical Pacific Ocean computed from subsurface ocean data and wind stress data. Deep-Sea Research 1987; 34: 33-43.
49. Dietrich G. *General Oceanography - an Introduction*. John Wiley & Sons, Inc: New York, 1963; 74-188.
50. Sukhatme SP, Nayak JK. *Solar Energy – Principles of thermal collection and storage*. Tata – McGraw Hill: New Delhi, 2008; 74 – 78.

51. National Snow and Ice Center. *Shortwave radiation*. Available from: http://nsidc.org/arcticmet/glossary/short_wave_radiation.html. Accessed on 13.04.2010.
52. Stevenson JW, Niler PP. Upper Ocean Heat Budget During the Hawaii-to-Tahiti Shuttle Experiment. *Journal of physical oceanography* 1983; 13: 1894 -1907.
53. Duxbury AB, Duxbury AC, Sverdrup KA. *Fundamentals of Oceanography*. McGraw-Hill Companies: New York, 2002; 125-126.
54. Curry JA, Webster PJ. *Thermodynamics of atmosphere and oceans*. Academic Press: UK, 1999; 331 – 335.
55. *Solar Constant*. Available from: http://dictionary.reference.com/browse/solar+constant?jss=1. Accessed on 13.04.2010.
56. Pickard GL, Emery WJ. *Descriptive Physical Oceanography, 5th edition*. Pergamon Press: Great Britain, 1990; 39 – 82.
57. Kininmonth W. *Climate Change: a natural hazard*. Multi –Science Publishing: UK, 2004; 76 – 81.
58. Pyranometer. Available from: http://www.global-greenhouse-warming.com/pyranometer.html. Accessed on 13.04.2010.
59. Rohli RV, Vega AJ. *Climatology*. Jones and Bartlett Learning: UK, 2008; 91-97.
60. Laevastu T. *Energy exchange in the North Pacific; its relations to weather and its oceanographic consequences*. Hawaii Inst. Geophysics 1963; Report 29: 15.
61. *Okta*. Available from: http://en.wikipedia.org/wiki/Okta. Accessed on: 15.06.2010.
62. Bryden HL. *Ocean Heat Transport*. Available from: http://www.ocean.washington.edu/people/faculty/luanne/classes/pcc586/papers/brydenn.pdf. Accessed on 22.06.2010.
63. *Radiometer*. Available from: http://en.wikipedia.org/wiki/Radiometer. Accessed on 13.04.2010.
64. Angel MV. *The pelagic Environment of the Open Ocean*. In: Tyler P, editor. Ecosystems of the deep oceans. Elsevier Science: Netherlands, 2003; 39 – 80.
65. Strahler A, Strahler A. *Introducing Physical Geography, 4th edition*. John Wiley and Sons: Hoboken, 2006; 68.

66. Hartman DL. *Global physical climatology*. Academic Press: USA, 1994; 102 - 105.
67. Husick CB. *Chapman piloting and seamanship, 66th edition*. Hearst Books: New York, 2009; 803.
68. Ahrens CD. *Essentials of meteorology – an invitation to the atmosphere, 5th edition*. Thomson Brooks/Cole: USA, 2008; 305-306.
69. Lykossov VN. *Atmospheric and oceanic boundary layer physics*. In: Jones ISF, Toba Y, editors. Wind stress over the ocean. Cambridge University Press: USA, 2001; 54 – 81.
70. Ginis I. New *strategies for comprehensive coupled atmosphere-ocean-wave modeling in tropical cyclones*. Available from: http://www.cawcr.gov.au/bmrc/basic/cawcr-wksp2/papers/Ginis.pdf. Accessed on 18.07.2010.
71. Andreas EL. *An algorithm to predict the air-sea fluxes in high-wind, spray conditions*. Available from: ams.confex.com/ams/pdfpapers/52221.pdf. Accessed on 18.07.2010.
72. Pinet PR. *Invitation to oceanography, 3rd edition*. Jones and Bartlett Publishers: UK, 2003; 151 – 156.
73. Lewis WM (Jr.). Tropical Limnology. *Annual Review of Ecology and Systematics* 1987; 18:159 – 184.
74. Brink KH, Robinson AR. *Global coastal ocean, the: regional studies and syntheses*. Harvard University Press: USA, 2005; 20-25.
75. Hastenrath S. Heat budget of Tropical Ocean and Atmosphere. *Journal of Physical Oceanography* 1980; 10: 159 – 170
76. Chapin (III) SF, Matson PA, Mooney HA. *Principles of terrestrial ecosystem ecology*. Springer Science + Business Media, Inc.: USA, 2002; 28 – 31.
77. Zhang Y, Rossow WB, Stackhouse P (Jr.), Romanou A, Wielicki BA. Decadal variations of global energy and ocean heat budget and meridional energy transports inferred from recent global data sets. *Journal of geophysical research* 2007; 112: doi: 10.1029/2007JD008435
78. Allen PA. *Earth Surface Processes*. Wiley – Blackwell: Hoboken, 1997; 19 – 27.
79. Finney KA. Ocean Thermal Energy Conversion. *Guelph Engineering Journal (1)* 2008, 17-23, ISSN: 1916-1107

80. 2010 Offshore Infrastructure Associates, Inc. *History of OTEC*. Available from: http://www.offinf.com/history.htm. Accessed on 20.07.2010.
81. Takahashi PK, Trenka A. *Ocean Thermal Energy Conversion*. John Wiley & Sons: Chichester, 1996; 1-5
82. Chiles RJ. *The Other Renewable Energy*. Available from: http://www.clubdesargonautes.org/energie/chiles.pdf . Accessed on 23.12.2010.
83. Advanced technology group. *Ocean thermal energy conversion*. Available from: http://www.oocities.com/pemnq/oceanthermalscan.pdf. Accessed on: 19.12.2010.
84. Cohen R. Energy from the ocean. *Phil. Trans. R.Soc.Lond.A* 1982; 307: 405-437.
85. Binger A. *Potential and Future Prospects for Ocean Thermal Energy Conversion (OTEC) In Small Islands Developing States (SIDS*). Available from: www.sidsnet.org/docshare/energy/20040428105917_otec_un.pdf. Accessed on 20.08.2010.
86. National Renewable Energy laboratory. *Ocean thermal energy conversion – electricity production*. Available from at: http://www.nrel.gov/otec/electricity.html. Accessed on: 29.04.2010.
87. Tony W, Twidell J. *Renewable Energy Resource, 2nd edition*. Taylor and Francis: London, 2006; 451-470.
88. Nihous GC. An estimate of Atlantic Ocean thermal energy conversion (OTEC) resources. *Ocean Engineering* 2007; 34: 2210-2221.
89. Uehara H, Dilao CO, Nakaoka T. Conceptual Design of Ocean Thermal Energy Conversion (OTEC) Power Plants in the Philippines. *Solar Energy* 1988; 41: 431-441.
90. Yamada N, Hoshi A, Ikegami Y. Thermal Efficiency Enhancement of Ocean Thermal Energy Conversion (OTEC) using Solar Thermal Energy. *4th International Energy Conversion Engineering Conference and Exhibit (IECEC)*, San Diego, California, American Institute of Aeronautics and Astronautics, 2006-4130.
91. Tong W, Liang D, Chuangang GU, Bo Y. Performance analysis and improvement for CC-OTEC system. *Journal of Mechanical Science and Technology* 2008; 22: 1977-1983.

92. Straatman PJT, Sark WGJHM. A new hybrid ocean thermal energy conversion-Offshore solar pond (OTEC-OSP) design: A cost optimization approach. *Solar Energy* 2008; 82: 520-527.

93. Gupta MK, Kaushik SC. Exergetic utilization of solar energy for feed water preheating in a conventional thermal power plant. *International Journal of Energy Research* 2009; 33:593-604.

94. Ravindran, M.; Abraham R. The Indian 1 MW demonstration OTEC plant and the development activities. *OCEANS '02 MTS/IEEE* 2002; 3: 1622- 1628. doi: 10.1109/OCEANS.2002.1191877

95. Magesh R. OTEC technology – A world of clean energy and water. In: *Proceedings of the World Congress on Engineering 2010 Vol II WCE 2010*, London UK, 2010.

96. Asou H, Yasunaga T, Ikegami Y. Comparison between Kalina Cycle and Conventional OTEC System using Ammonia-Water Mixtures as Working Fluid. In: *Proceedings of the Seventh (2007) international Offshore and Polar Engineering Conference* Lisbon, Portugal, The International Society of Offshore and Polar Engineers (ISOPE); 2007. ISBN 978-1-880653-68-5; ISBN 1-880653-68-0(Set); ISSN 1098-6189(Set).

97. Rogdakis ED. Thermodynamic Analysis, Parametric Study and Optimum operation of the Kalina Cycle. *International Journal of Energy Research* 1996; 20: 359-370.

98. Kim NJ, Ng KC, Chun W. Using the condenser effluent from a nuclear power plant for Ocean Thermal Energy Conversion (OTEC). *International Communications in Heat and Mass Transfer* 2009; 36: 1008-1013.

99. Sørensen B. A sustainable energy future: Construction of demand and renewable energy supply scenarios. *International Journal of Energy Research* 2007; 32: 436-470.

100. *2004 Survey of Energy Resources 20th edition*. World Energy Council, Elsevier 2004; 419 – 432.

101. Valis GK. *Atmospheric and oceanic fluid dynamics, fundamentals and large scale circulation*. Cambridge University Press: 2006; 667 – 671.

102. *Taking the oceans temperature.* Available from: http://er.jsc.nasa.gov/seh/Ocean_Planet/activities/ts2ssac4.pdf. Accessed on: 6.09.2010.
103. Ikegami I. *Ocean Thermal Energy – to transform our lives*. International Symposium on Renewable Energy, USP, Fiji. Available from: http://www.usp.ac.fj/index.php?id=9161 . Accessed on: 25.11.2010.
104. Tomczak M. *Thermohaline processes; water mass formation; the seasonal thermocline*. Available from: http://www.incois.gov.in/Tutor/IntroOc/lecture07.html. Accessed on: 2.10.2010.
105. *Navy operational ocean circulation and tide models*. Available from: http://www.oc.nps.edu/nom/day1/parta.html. Accessed on: 13.10.2010.
106. Stewart RH. *Chapter 6 - Temperature, Salinity, and Density*. Available from: http://oceanworld.tamu.edu/resources/ocng_textbook/chapter06/chapter06_05.htm Accessed on 29.04.2010.
107. Lynne Talley. *SIO 210 Talley Topic: Properties of seawater*. Available from at: http://sam.ucsd.edu/sio210/lect_2/lecture_2.html. Accessed on: 3.12.2010.
108. *Potential Temperature*. Available from: http://en.wikipedia.org/wiki/Potential_temperature. Accessed on: 28.04.2010.
109. Gregory J. Vertical heat transports in the ocean and their effect on time-dependent climate change. *Climate Dynamics* 2006; 16: 501 – 515.
110. Hamilton K. *Numerical resolution and modeling of the global atmospheric circulation: A review of our current understanding and outstanding issues*. In: Hamilton K, Ohfuchi W, editors. High resolution numerical modelling of the atmosphere and ocean. Springer: New York, 2008; 7 – 22.
111. Lansberg HE, Miegham JV. *Advances in geophysics, Vol. 10*. Academic Pres: London, 1964; 8 – 9.
112. Summerhayes CP, Thorpe SA. *Oceanography, an illustrated guide*. Manson Publishing Ltd.: London, 1996; 29 – 32.
113. Yeh RH, Su TZ, Yang MS. Maximum output of an OTEC power plant. *Ocean Engineering* 2005; 32: 685-700.

114. Uehara H, Ikegami Y. Optimization of a Closed-Cycle OTEC System. Trans ASME Journal of *Solar Energy Engineering* 1990; 112: 112-256.

115. Mukherjee D, Chakrabari S. *Fundamentals of renewable energy systems*. New Age International (P) Ltd.: New Delhi, 2004; 193 – 197.

116. *Ocean Thermal Energy Conversion*. Available from: http://en.wikipedia.org/wiki/Ocean_thermal_energy_conversion. Accessed on: 29.04.2010.

117. Uehara H, Miyara A, Ikegami Y, Nakaoka T. Performance Analysis of an OTEC Plant and a Desalination Plant Using an Integrate Hybrid Cycle. *Trans ASME Journal of Solar Energy Engineering* 1996; 118: 115-122.

118. Uehara H, Nakaoka T. *Development and prospective of ocean thermal energy conversion and spray flash evaporator desalination*. Available from: http://www.ioes.saga-u.ac.jp/VWF/general-review_e.html. Accessed on: 14.09.2010.

119. Crews R. *OTEC Sites*. Available from: http://www.trellis.demon.co.uk/reports/otec_sites.html. Accessed on: 23.11.2010.

120. National renewable Energy Laboratory. *Ocean Thermal Energy Conversion – Plant Design and Location*. Available from: http://www.nrel.gov/otec/design_location.html. Accessed on: 29.04.2010.

121. Wang SK, Hung TC. Renewable Energy from the Sea – Organic Rankine Cycle using Ocean Thermal Energy Conversion. *PEA-AIT International Conference on Energy and Sustainable Development: Issues and Strategies (ESD 2010),* Chiang Mai, Thailand, 2010.

122. Vega LA. *OTEC news – OTEC review*. Available from: http://www.otecnews.org/articles/vega/10_potential_locations.html. Accessed on 03.07.2010.

123. Rupeni M. Ocean Thermal Energy Conversion and the Pacific Islands. *SOPAC miscellaneous report 417*. Fiji: South Pacific Applied Geoscience Commission (SOPAC), 2001.

124. Odum HT. Emergy evaluation of an OTEC electrical power system. *Energy* 2000; 25: 389-393.

125. Nihous GC, Syed MA. A Financing Strategy for Small OTEC Plants. *Energy Conversion Management* 1997; 38: 201-211.

126. Srinivasan N, Sridhar M, Agrawal M. Study on the Cost Effective Ocean Thermal Energy Conversion. *Offshore Technology Conference*, Texas, USA, 2010.

127. *Ocean Thermal Energy Conversion*. Available from: www.123eng.com/seminar/Ocean%20thermal%20energy%20conversion.pdf Accessed on: 23.11.2010.

128. Lennard DE. The Viability and Best Locations for Ocean Thermal Energy Conversion Systems Around the World. *Renewable Energy* 1995; 6: 359-365.

129. *Ocean thermal energy conversion – going deeper into renewables*. Available from: http://mae.ucdavis.edu/faculty/erickson/EnergyConversion/OTEC_final_files/frame.htm. Accessed on: 15.12.2010.

130. Ertekin RC, Qian ZM, Nihous GC, Vega LA, Yang C. Positioning of a Floating OTEC Plant by Surface Intake Water. The International Society of Offshore and Polar Engineers, *International Journal of Offshore and Polar Engineering* 1993; 3: ISSN: 1053-5381.

131. McHale A, Jones W L, Horn HM. Deployment and operation of the 50 kW mini-OTEC plant, OTC 3686. *Offshore technology conference,* Houston, 1980.

132. McHale F. Construction and deployment of an operational OTEC plant at Kona, Hawaii, OTC 3545. *Offshore technology conference,* Houston, 1979.

133. Mitsui T, Ito F, Seya Y, Nakamoto Y. Outline of the 100 kW OTEC pilot plant in the republic of Nauru. *IEE transactions on power apparatus and systems*, 1983; PAS-102: 3167-3171.

134. Pillai IR, Banerjee R. Renewable energy in India: Status and potential. *Energy*, 2009; 34: 970-980.

135. Kobayashi H, Jitsuhara S, Uehara H. *The present status and features of OTEC and real aspects of thermal energy conversion technologies*. Available from: http://www.nmri.go.jp/main/cooperation/ujnr/24ujnr_paper_jpn/Kobayashi.pdf. Accessed on: 30.03.2011.

136. Plocek TJ, Laboy M. Ocean Thermal Energy Conversion (OTEC): Technical Viability, Cost Projections and Development Strategies. *Offshore Technology Conference*, Texas, USA, 2009.

137. Guo-Yan Z, En W, Shan-Tung T. Techno-economic study on compact heat exchangers. *International Journal of Energy Research,* 2008; 32: 1119-1127.

138. Vega LA. Ocean Thermal Energy Conversion Primer. *Marine Technology Society Journal*, 2002/2003; 6: 25-35.

139. Vadus JR, Taylor BJ. OTEC cold water pipe research. *IEEE Journal of oceanic engineering*, 1985; OE -10: 114 – 122.

140. William J, Krömer G, Weingart J. *Climate and solar energy conversion*. International Institute for Applied Systems Analysis: Austria, 1978; 4 – 9.

141. Komiyama H, Yamada K. Ecosystem Driven by OTEC and Oceanic High Mineral Water – Otohime Project-. *Energy Conversion Management* 1995; 36: 889-894.

142. Sansone F, Weng K. *Hawaii national marine renewable energy center - environmental impact studies*. Available from: http://hinmrec.hnei.hawaii.edu/ongoing-projects/environmental-impact-studies/. Accessed on: 15.12.2010.

143. *Ocean Thermal Energy Conversion (OTEC) Environmental Impacts*. Available from: http://coastalmanagement.noaa.gov/otec/docs/environmentalfactsheet.pdf. Accessed on: 15.12.2010.

144. Jirka GH, Fry DJ, Johnson RP, Harleman DRF. Ocean thermal energy conversion: experimental and analytical study of mixing and recirculation. *Energy laboratory report No. MIT-EL 77-011*, 1977.

LIST OF FIGURES

LIST OF TABLES

Mohammed Faizal_Figure 1

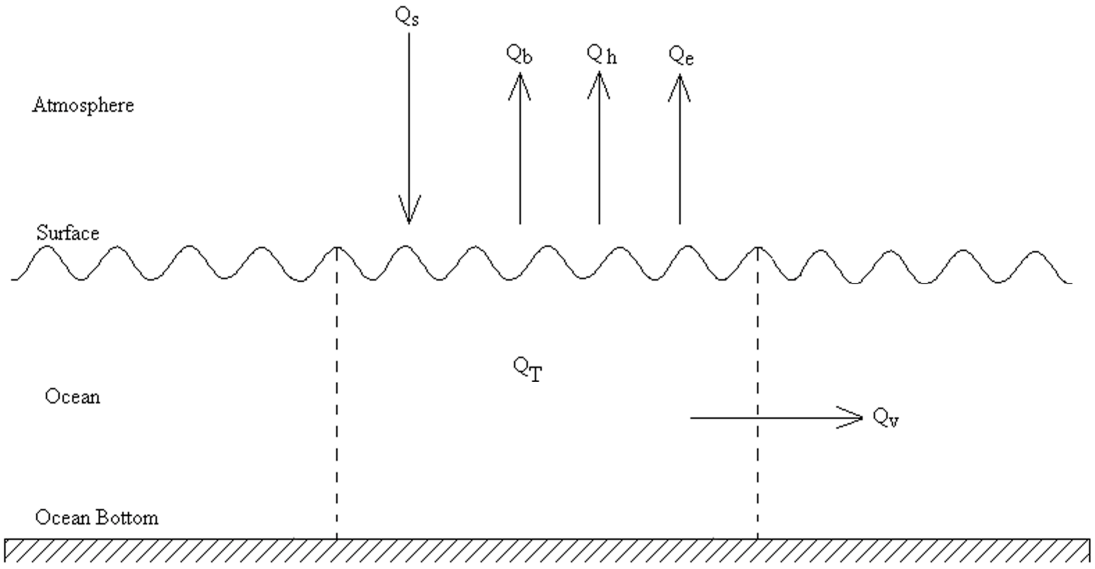

Figure 1. Schematic diagram of heat transfer processes from a given area of the ocean [41].

Mohammed Faizal_Figure 2

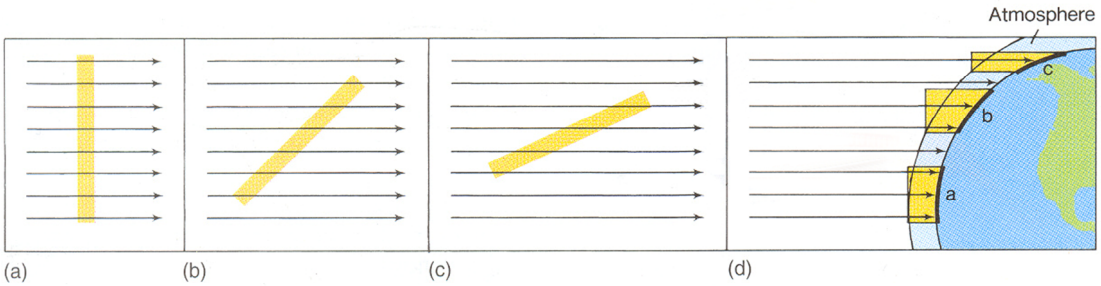

Figure 2. The earth's surfaces that are equal in size at different latitudes receive different levels of solar radiation because of different angles at which sunlight strikes the earth [51].

Mohammed Faizal_Figure 3

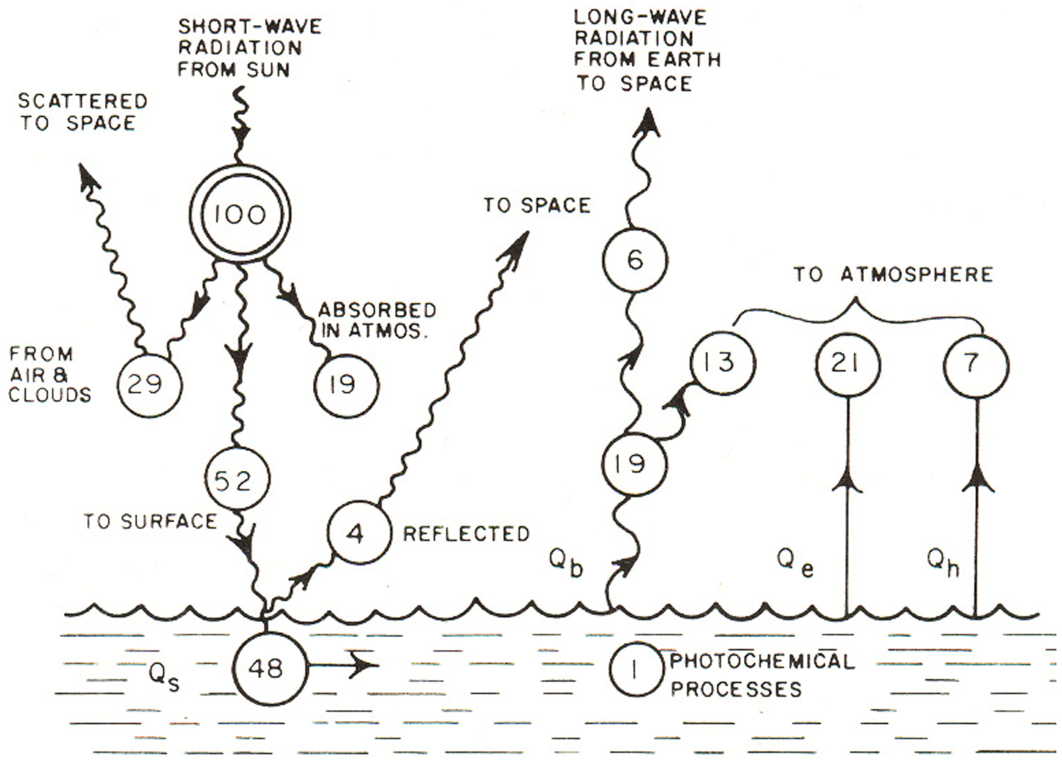

Figure 3. The average heat budget of the ocean in terms of 100 units of incoming radiation, associated disturbances in the atmosphere, and reflections from the surface [54].

Mohammed Faizal_Figure 4

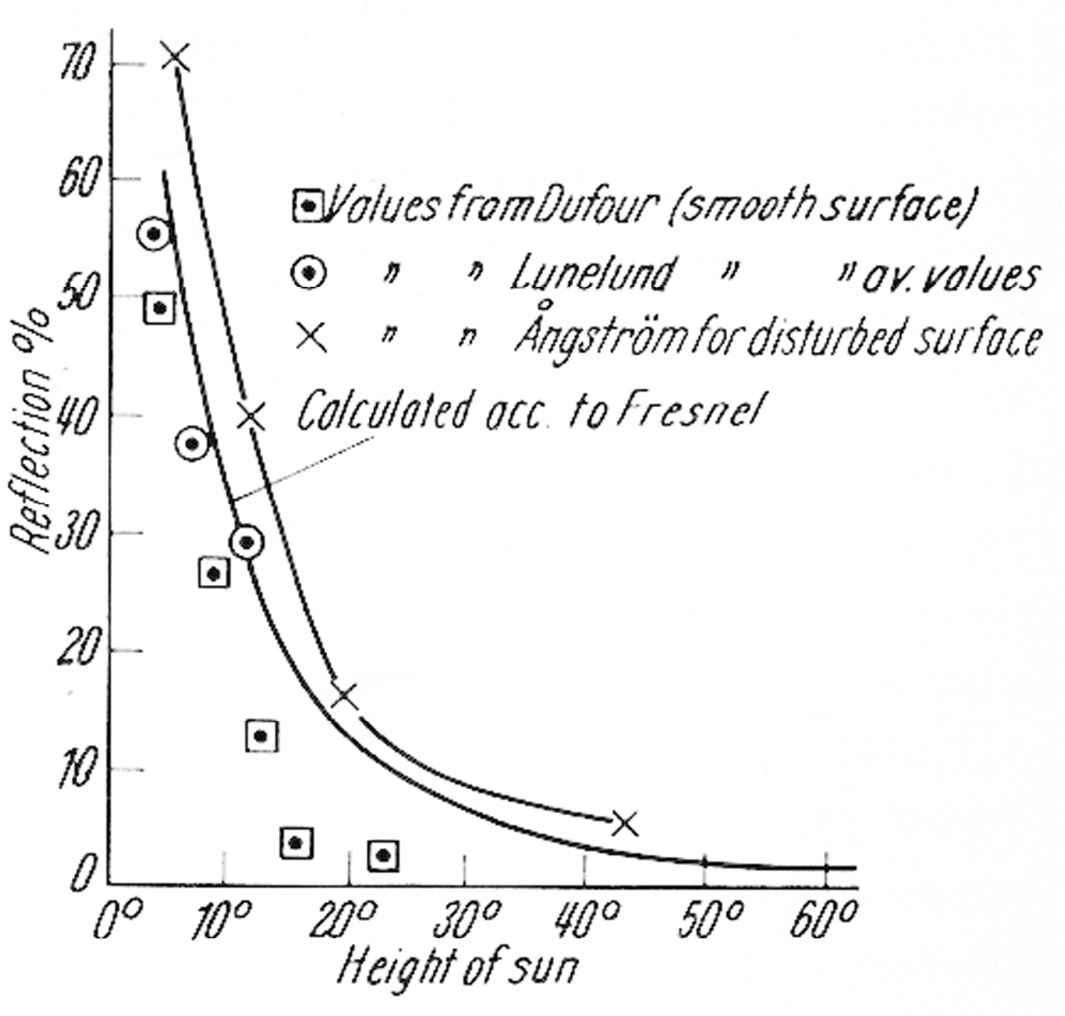

Figure 4. Reflection of solar radiation at different sun altitudes [49].

Mohammed Faizal_Figure 5

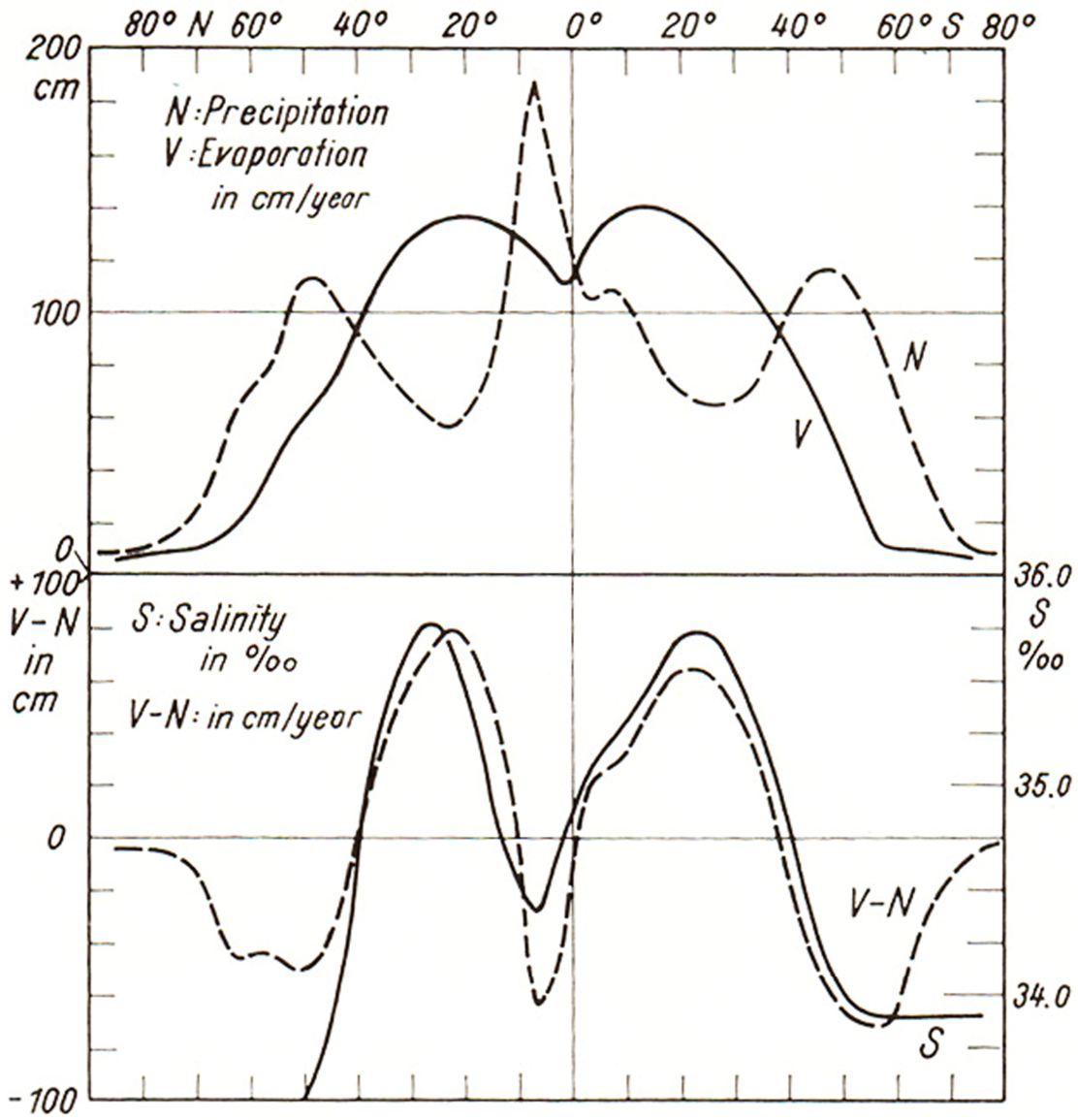

Figure 5. Precipitation *N*, evaporation *V*, *V-N*, and salinity S distribution at different latitudes [47].

Mohammed Faizal_Figure 6

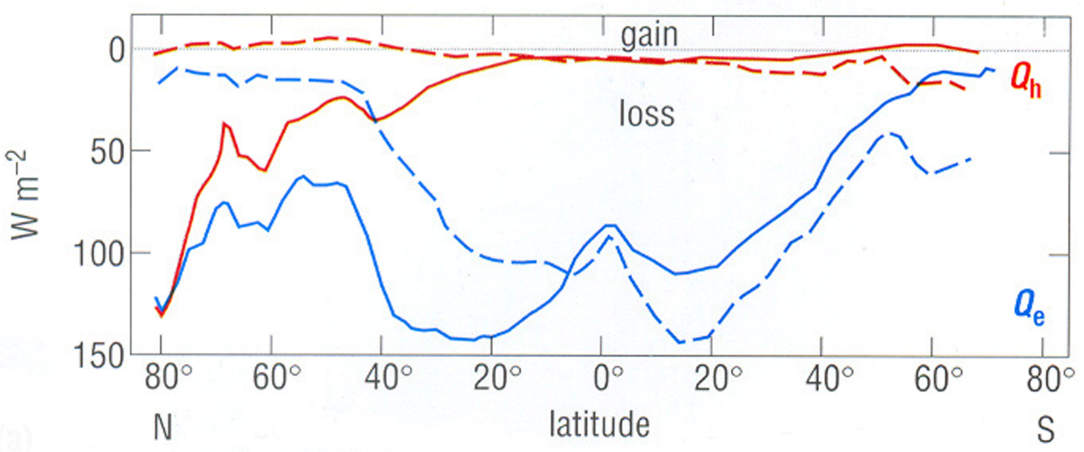

Figure 6. The Q_h and Q_e terms at different latitudes. B increases with increasing latitudes [38].

Mohammed Faizal_Figure 7

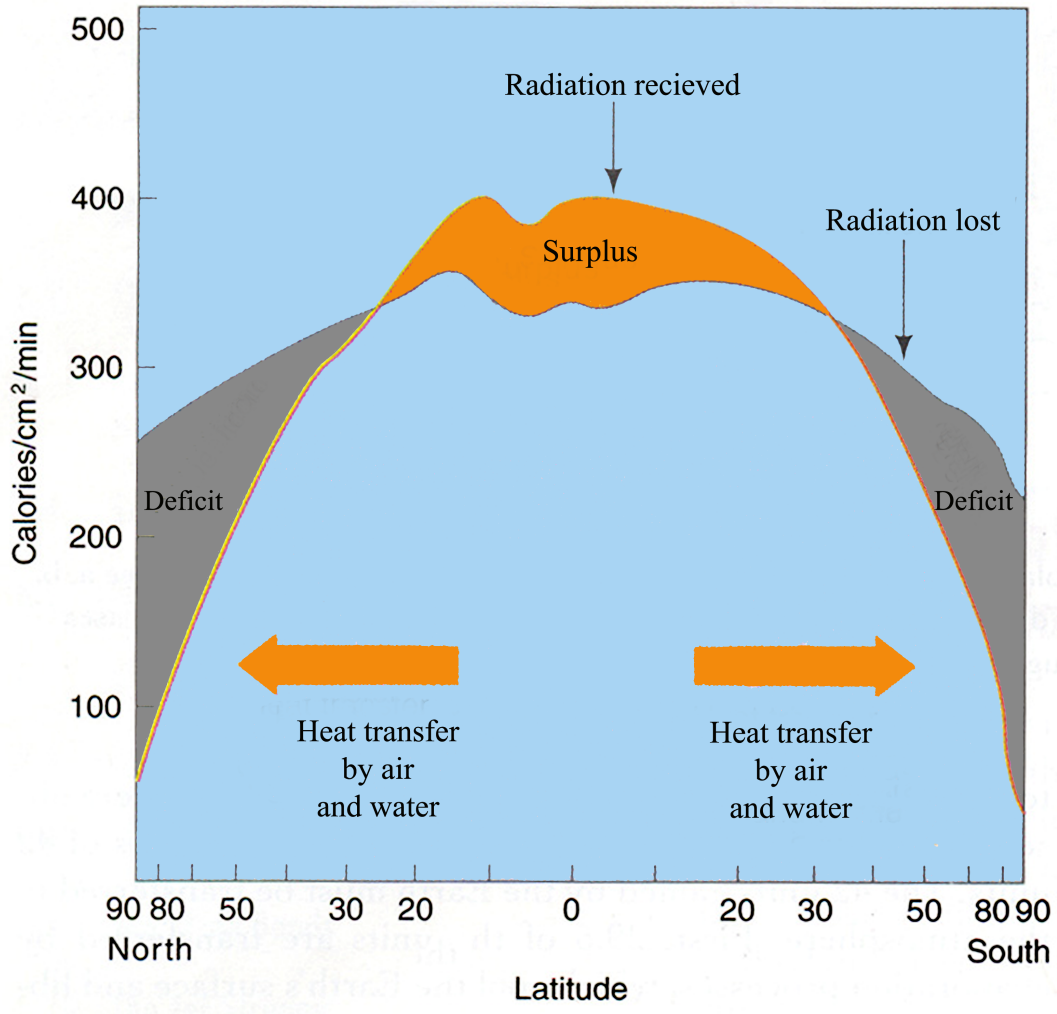

Figure 7. Comparison of the amount of radiation received at different latitudes [51].

Mohammed Faizal_Figure 8

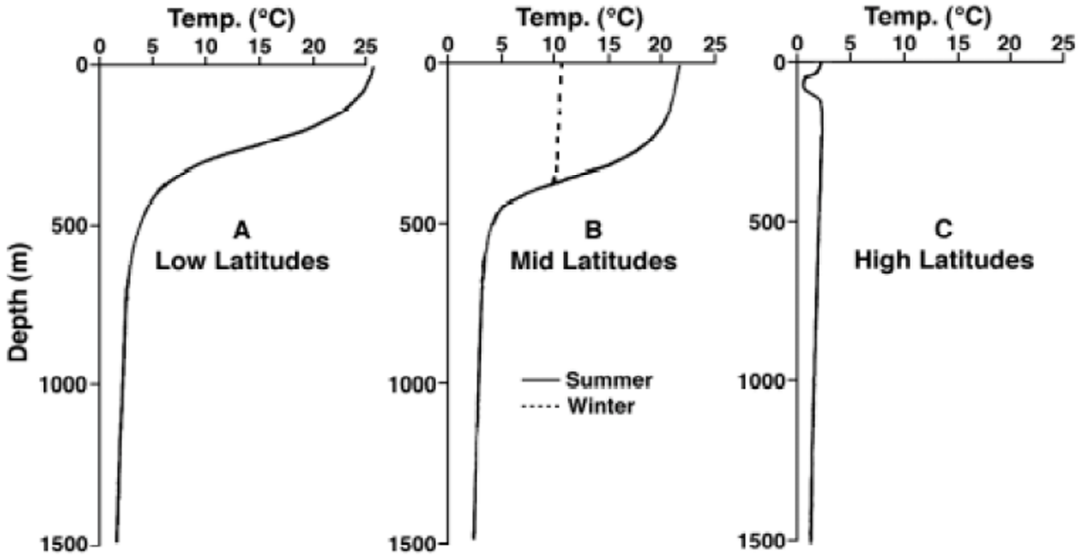

Figure 8. Typical mean temperature vs. depth profiles of the open ocean at different latitudes [101].

Mohammed Faizal_Figure 9

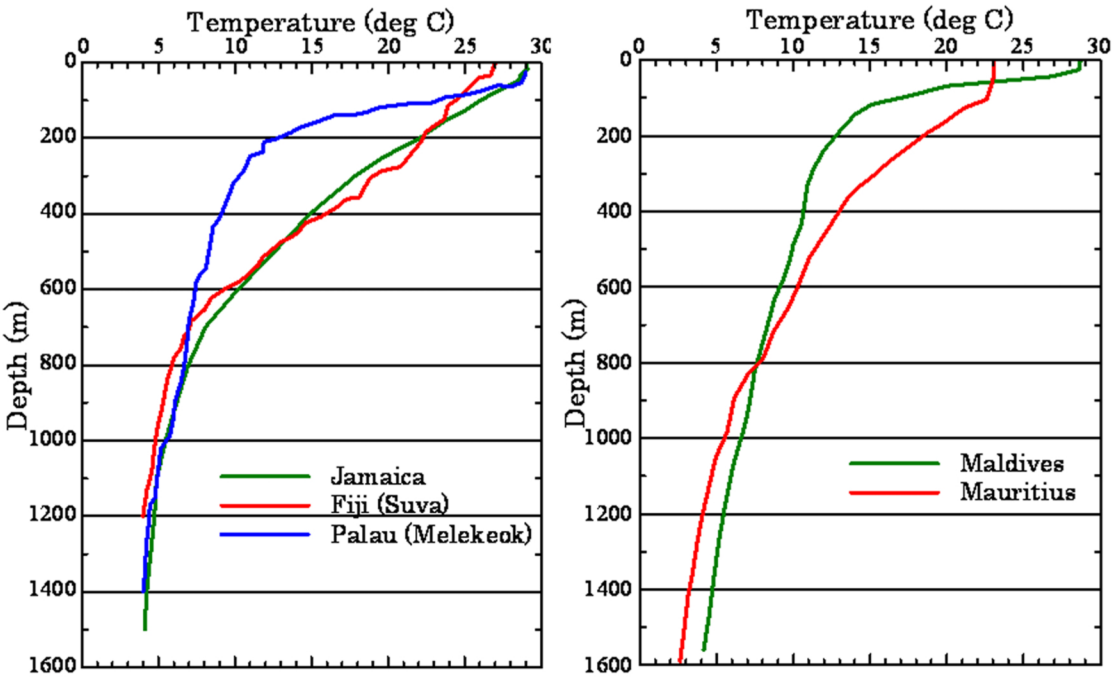

Figure 9. Typical mean temperature vs. depth profiles for some countries [102].

Mohammed Faizal_Figure 10

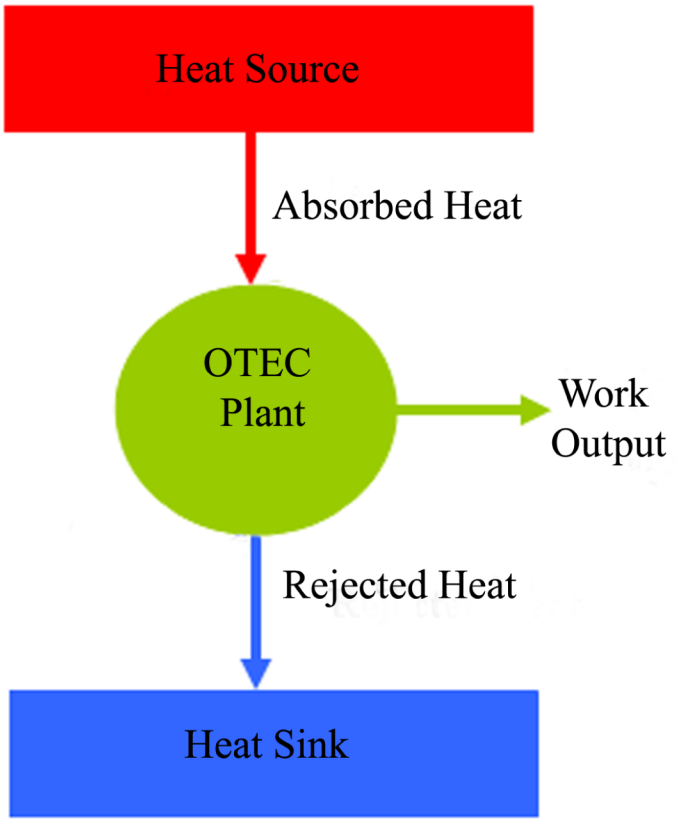

Figure 10. Schematic diagram of an OTEC plant operating as a heat engine.

Mohammed Faizal_Figure 11

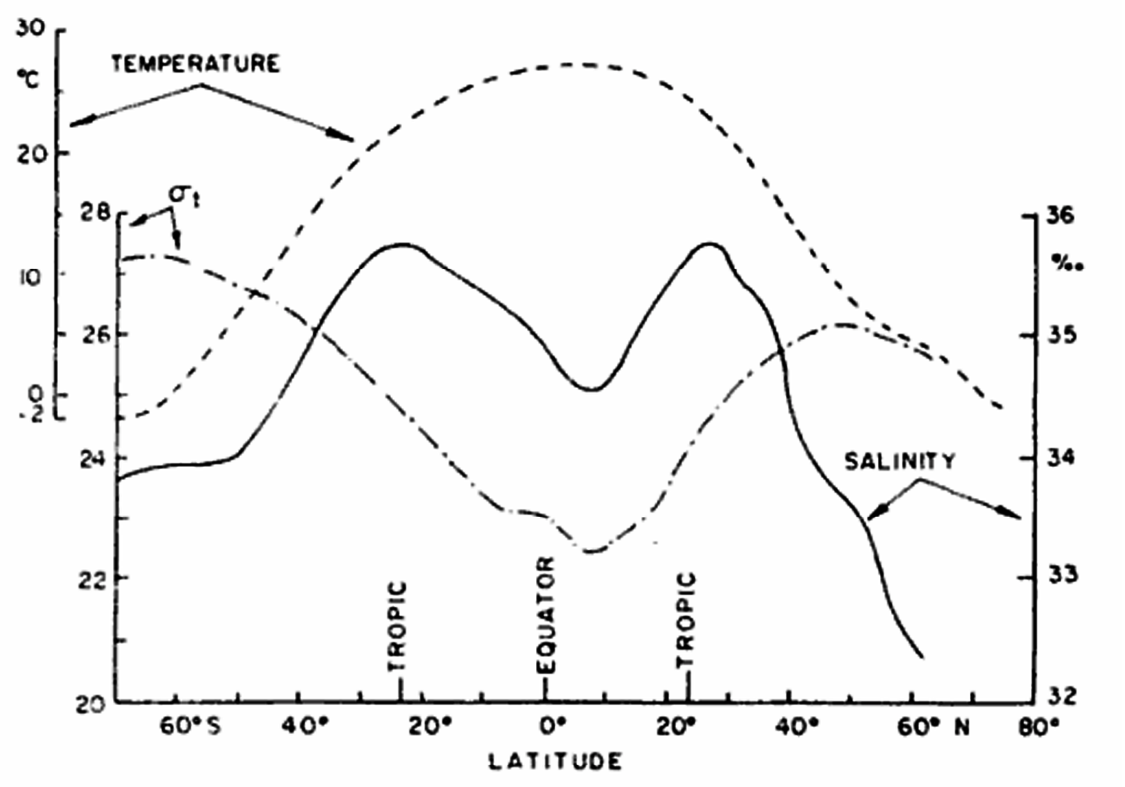

Figure 11. Latitudinal variation of surface temperature, salinity and density (σ_t) average for all oceans [54].

Mohammed Faizal_Figure 12

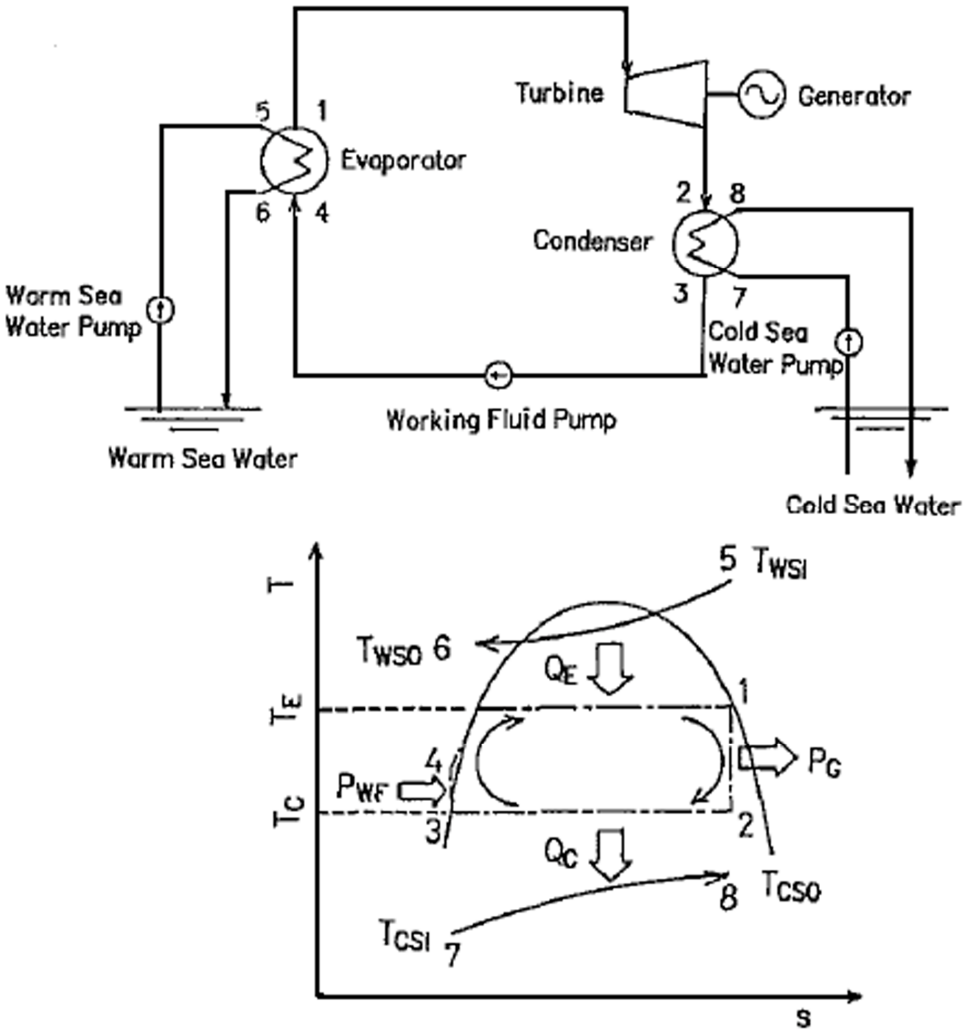

Figure 12. Schematic diagram of a closed cycle OTEC system and its T-S diagram [112].

Mohammed Faizal_Figure 13

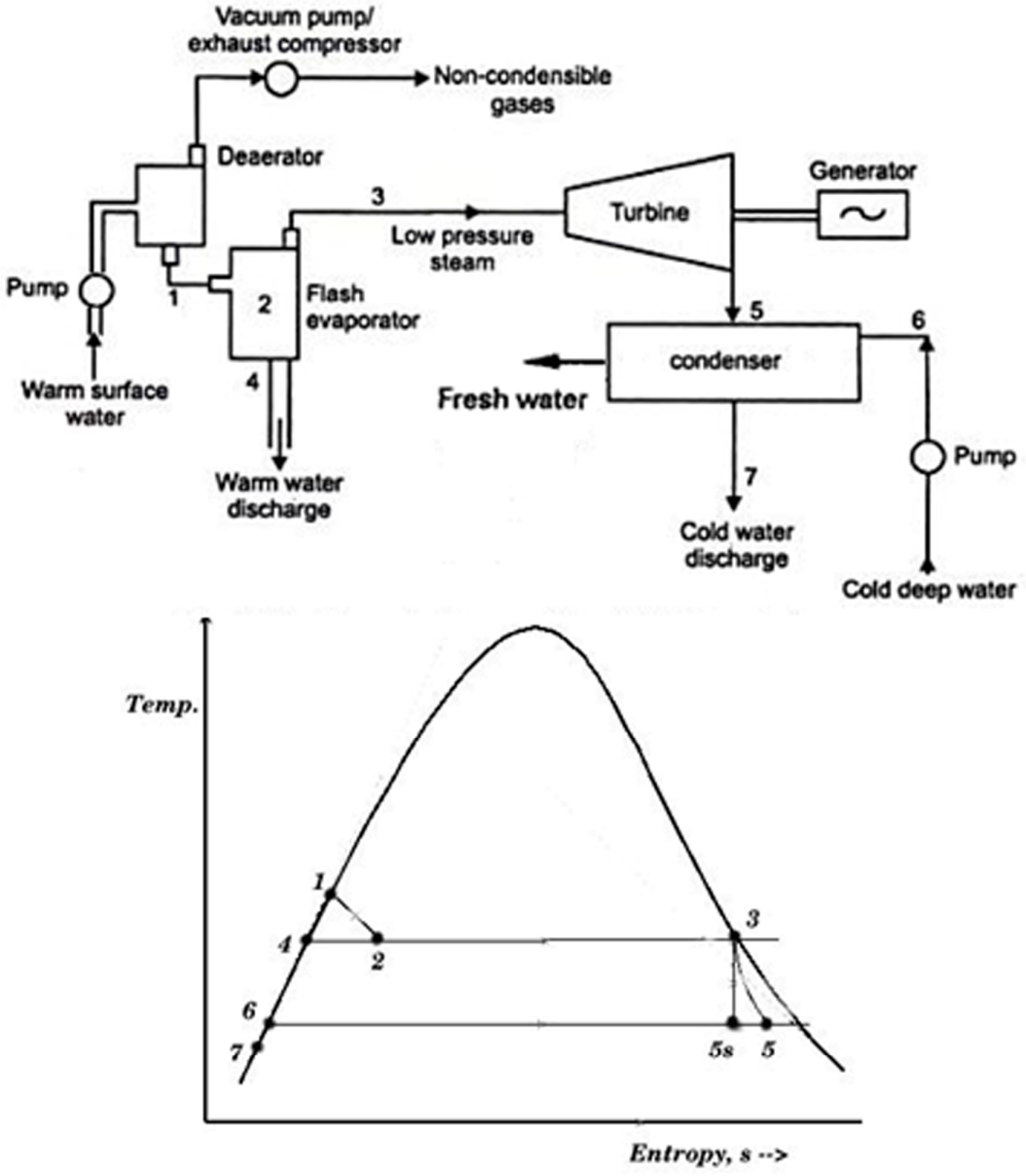

Figure 13. Schematic diagram of an open cycle OTEC system and its T-S diagram [113,114].

Mohammed Faizal_Figure 14

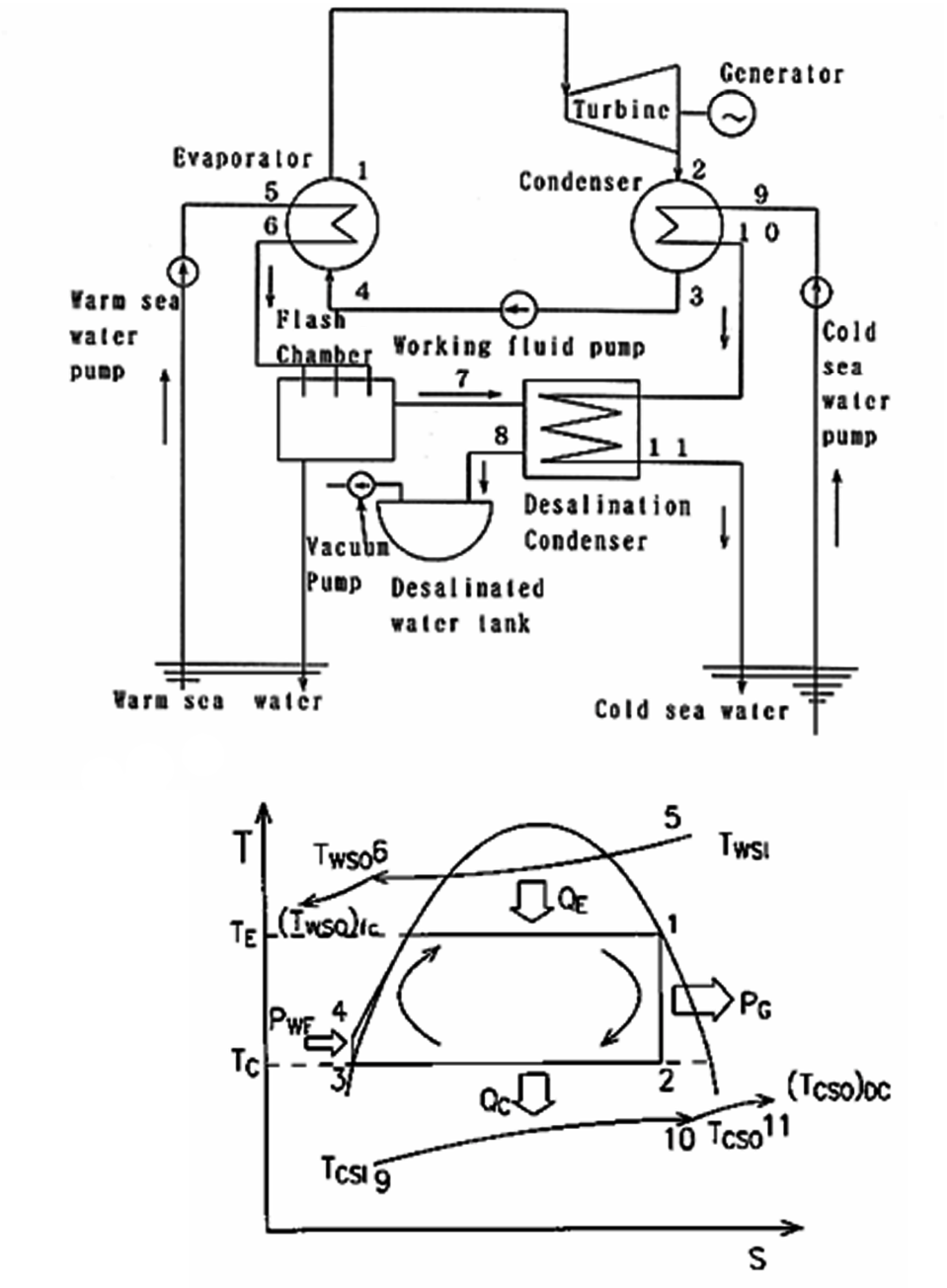

Figure 14. Schematic diagram of a hybrid cycle OTEC system and its T-S diagram [115,116].

Table1

Country/Area	**Temperature Difference (ºC) between the surface water and water at a depth of 1000 m**	**Distance from Resource to Shore (km)**
Africa		
Benin	22-24	25
Gabon	20-22	15
Ghana	22-24	25
Kenya	20-21	25
Mozambique	18-21	25
São Tomé and Prí-ncipe	22	1-10
Somalia	18-20	25
Tanzania	20-22	25
Latin America and the Caribbean		
Bahamas, The	20-22	15
Barbados	22	1-10
Cuba	22-24	1
Dominica	22	1-10
Dominican Republic	21-24	1
Grenada	27	1-10
Haiti	21-24	1
Jamaica	22	1-10
Saint Lucia	22	1-10
Saint Vincent and the Grenadines	22	1-10

Trinidad and Tobago	22-24	10
U.S. Virgin Islands	21-24	1
Indian and Pacific Oceans		
Comoros	20-25	1-10
Cook Islands	21-22	1-10
Fiji	22-23	1-10
Guam	24	1
Kiribati	23-24	1-10
Maldives	22	1-10
Mauritius	20-21	1-10
New Caledonia	20-21	1-10
Pacific Islands Trust Territory	22-24	1
Philippines	22-24	1
Samoa	22-23	1-10
Seychelles	21-22	1
Solomon Islands	23-24	1-10
Vanuatu	22-23	1-10